Response to Reviewer 1: Reviewer comments are reproduced in bold font and author comments in regular typeface.

Review of "Ice nucleation properties of K-feldspar polymorphs and plagioclase feldspars" by André Welti and co-authors for Atmospheric Chemistry and Physics

General comments:
Welti et al. present a study about the immersion freezing behavior of a variety of different feldspar samples which builds on recent investigations by Augustin-Bauditz et al. (2014), Peckhaus et al., 2016), Harrison et al. (2016), and Whale et al. (2017). The samples were chosen carefully to provide a variety of crystal structures, chemical compositions, and ordering of the crystal lattice. They include five polymorphs of K-feldspar and four plagioclase feldspars. The immersion freezing experiments were performed with droplets containing single, size-selected particles and care was taken to minimize the amount of multiply-charged particles in the sample aerosol. Furthermore, the study includes X-ray fluorescence measurements giving information about bulk chemical composition and scanning electron microscopy images of particle morphology.

What differentiates the present paper from the earlier studies is the discussion of the effect of particle size and the degree of order in the crystal network on the ice nucleation efficiency of the samples. The authors' conclusions concerning these factors are generally comprehensible and well substantiated by the presented results. However, in some cases, which are pointed out in the specific comments, I am missing a more precise explanation. The figures are mostly clear, but I would like to suggest some alternatives for presenting the data (see specific comments). Language-wise, the paper is concisely written but some minor adjustments would increase readability (see technical corrections).
Overall, the paper is interesting, understandable, and fits within the scope of Atmospheric Chemistry and Physics. I recommend publication after minor editing.

We thank the reviewer for the comments and suggestions. We address the specific comments individually below.

Specific comments:
1) Size dependence of ice nucleation behavior

The authors often refer to the "pronounced size dependence of ice nucleation activity" as if this is a rarely observed feature. Normally, the ice nucleation behavior scales with the surface area of the immersed particles, meaning that the efficiency increases with increasing particle size. The authors should clarify to what extent the size dependent ice nucleation behavior of their samples deviates from the standard. In my opinion, this is best done by calculating the ice nucleation active surface site density $n_s(T)$ for differently sized particles. In contrast to the chosen T_{50} approach, this method would have the benefit of providing an overview over the whole investigated temperature range. I hence suggest to replace Fig. 5 with a multi-panel figure (like Fig. 3) showing $n_s(T)$ of the different particle sizes for all investigated samples (see, e.g., Fig. 5 in Hartmann et al., 2016).

We prefer to leave Figure 5 as is, but now add a figure in the appendix for the INAS densities since converting the frozen fraction to INAS densities involves accounting for the surface area, which is easily calculated given the particle size information in the manuscript. Concerning the extent of size dependence, we observe that all samples show a size dependence, mostly even stronger than linearly scaling with surface area with decreasing particle size. One microcline sample shows almost linear scaling of the frozen fraction with surface area. As all samples have this strong size dependence, we indeed consider it "pronounced". To be more specific we changed the sentence to (page 1 line 21-23): "A pronounced size dependence of ice

nucleation activity for the feldspar samples is observed, with the activity of smaller sized particles scaling with surface area or being even higher compared to larger particles. The size dependence varies for different feldspar samples."

Furthermore, the authors state that "microcline exhibited immersion freezing even for 50 nm particles" whereas for orthoclase "ice nucleation requires active sites present on 400-800 nm sized particles" and relate this observation directly to the effect of these particles on atmospheric ice nucleation. Concerning the potential of these species as atmospheric INP, one must always combine their efficiency and their abundance. Larger orthoclase particles might be needed to trigger ice nucleation as efficiently as smaller microcline particles, but maybe many more orthoclase particles are emitted into the atmosphere?

This is true, we agree, we have clarified this in the text, that atmospheric abundance of ice nucleation species needs to be considered in order to determine atmospheric relevance (see page 1 line 26-27)

Besides, the fact that ice nucleation was not observed for 100 or 200 nm orthoclase particles is related to the detection limit of the instrument. If the authors had investigated more droplets, they would eventually have observed ice nucleation triggered by the small orthoclase particles. This should be made clear in the manuscript.

We disagree with this reasoning, the argument of the detection limit applies to both, the orthoclase and the microcline experiments, the detection limit did not change between these two. i.e. we did not have to increase the amount of microcline in a single droplet, or increase the number of droplets observed in order to observe ice nucleation in the 50 nm microcline sample. The fact that 50 nm microcline (amazonite) demonstrated ice nucleation activity similar to that of 800 nm orthoclase, shows that even for the same detection limit, the 50 nm particles are potent INPs compared to the 100 or 200 nm orthoclase particles. i.e. by changing the number of droplets, or detection limit, this would not change the conclusions that 50 nm microcline particles are much more active than the 100 nm orthoclase particles.

2) Difference to earlier studies
This refers to P3L14-18, where I think the authors should clarify the innovation of their study more. Like this, it sounds as if they might expect an effect of methodology on the results, as the other studies were performed with droplets containing numerous particles each. Please state that by using single particles, you are focusing on a different temperature range than the other studies (except Augustin-Bauditz et al., 2014).

We have now clarified that we are able to focus on lower temperatures (< 253 K) with the single immersed particles (see page 3 line 30-31 in revised manuscript). However, the observed size dependence also indicates that except for cases where activity scales linearly with surface area (only one Microcline in this study), the particle size distribution used in drop freezing experiments (which make an assumption of linear scaling of activity with surface area) can potentially have an influence on the measured activity.

3) Multiply-charged particles
The authors should be more precise concerning the amount of multiply-charged particles in the cases where the CPMA was not used. This issue could be addressed by including actually measured size distributions in Fig. 2 instead of the schematic ones. Alternatively, the authors could include the following statement on P4L28-29: "The use of the CPMA for the selection of larger particles (400 nm, 800 nm) was not necessary as the fraction of larger particles was reduced to … % by the cyclones and the impactor upstream of the DMA."

We agree with the reviewer and now include specific numbers for the diameters and fraction of multiply charged particles in section 3.1 of the revised manuscript (see page 5 line 10 -22). We also include a figure in Appendix C to show the contribution of the multiply charged particles to the frozen fractions for the 50 nm sample, where the highest multiple charged particle fraction is calculated.

4) Figure 4

I see more benefit from one figure showing *FF* over *T* for 800 nm particles of all samples. This would be more suited for comparing the ice nucleation signatures of the different feldspars than just showing the range in which freezing occurred. Error bars could be omitted (because they are already shown in Fig. 3) and symbol size reduced for clarity.

Even without the error bars, such a figure becomes messy and actually rather difficult to read, as there is a huge amount of data overlap. It results in not being able to see the frozen fraction curves for many samples because of the temperature overlap. As such we keep Figure 4 as is. Furthermore, not having error bars if we plot frozen fraction vs. temperature would not allow for a realistic comparison of differences (or similarities) between the samples.

Technical corrections:

P1L9: Replace "Na/Ca-rich feldspar" with plagioclase to be consistent with the title. The composition is explained below anyhow.

We agree, done (page 1 line 9 revised manuscript)

P1L11: Replace "are" with "were" in "Samples are selected…".

Done (page 1 line 11)

P1L18-20: This sentence would benefit from being split into two.

We agree, done (page 1, line 18-19).

P1L24-25: Either omit the "s" at "temperatures" or at "depends".

We changed "depends" to "depend" (page 1 line 26).

P1L29: There is also contact freezing in which the contact causes nucleation, not an immersed particle.

We have now adjusted page 2 line 2 -5 to reflect contact nucleation as a mechanism in this explanation of freezing of supercooled drops.

P2L12: Within a sentence "e.g." should be preceded by a comma. A comma should also follow in case you are using American English. This also applies to "i.e.". Generally, check your manuscript for consistency with either British or American English. E.g., see "favouring" on P11L10 or "generalise" and "analysed" on P12L8 and L13.

We inserted the comma before "e.g." (page 2 line 17) but not after as we are using British English as is evident by the words specified by the reviewer.

P2L13: Less efficient in comparison to which other species?

Compared to other mineral species such as muscovite and kaolinite – we have now clarified this aspect on page 2 line 18 of the revised manuscript.

P2L14: Change "for example" to "e.g.".

Done, now page 2 line 19

P2L22: Capital "X" in "x-ray".
Done, now page 2 line 27

P3L21: Mention that XRF is a bulk, not a single particle technique.
We now mention this on page 4 line 3, in addition we note that we explicitly state that XRF is a bulk composition measurement when discussing the data in section 5.2, already in the original manuscript.

P3L28: Omit comma following "polymorphism" and add "s" to "occur".
Done, now page 4 line 10

P3L30-31: Add comma behind "sanidine". Be consistent using either "temperature" or "temperatures".
Comma added, and "temperatures" corrected to "temperature", page 4 line 12 in revised manuscript.

P4L1-2: I suggest to remove the brackets and structure the sentence as follows: "sanidine in volcanic and very high-temperature metamorphic rocks, orthoclase in … rocks and microcline in … rocks."
Done! Page 4 line 14-16 revised manuscript.

P4L2: "feldspar": This should be plural.
Changed to plural and added comma before feldspars (page 4 line 16)

P4L3: Why is Table 3 referred to before Table 2 is mentioned? Should the labels be switched?
Thank you for pointing this out. We now refer to section 5.2 (page 4 line 17) instead of Table 2.

P4L3-10: I appreciate the discussion of the atmospheric relevance of the samples. However, I feel that the last sentence in this paragraph might better be shifted before "We note…" to introduce the reader to this topic.
This has now been done. The last sentence "Samples used in this study.." has now been moved further up in the paragraph (Page 4 line 17-19 in revised manuscript). "We note" has now been changed to "As such.." (page 4 line 19)

P4L12: Change "are" to "were".
Done, page 4 line 26

P4L21: Change "multiple charged" to "multiply-charged", also in the other instances. Also, "single charged" should become "singly-charged".
This is a matter of preference, as such there is no rule saying multiple should be multiply etc. As such we retain the current structure. However, we note the lack of plurals on page 5 lines 4-5, and have corrected those.

P5L12: Remove hyphen in "ice-layer".
Done (now page 5 line 31)

P5L18: Insert hyphen in "in line".
Done (now page 6 line 4)

Fig. 3: Please state how you derived the error bars.
We have added a description of the error bars in the caption of Figure 3 and refer the interested reader to the work of Lüönd et al. (2010).

P6L13: How were the 25 % derived? Which particle size are you referring to?
Thanks for catching that, we were referring to the 800 nm particle curves in Figure 3. We have now corrected this (page 6 line 29).

P6L22-25: Could you state the parameters of the amazonite contact angle distribution? Should amazonite be capitalized on P6L22?
The parameters are the mean contact angle, and the variance of the distribution. However, the contact angle distribution referred to in page 7 line 11 is from a different paper (Ickes et al., 2017) and bears no inclusion here for just a single sample and is also not the focus or objective of the paper. We corrected the capitalization of amazonite on page 7 line 8 (revised manuscript) the reviewer is correct, this does not require capitalization. Thanks!

P6L26: Here you could refer to the Fig. showing $n_s(T)$ which I suggested as a replacement for Fig. 5.
We now refer to the INAS figure A1 in the appendix A (page 6, line 12-13).

P7L7-9: This statement would be more convincing if you provided actual numbers for the remaining multiply-charged particles in the 400 and 800 nm aerosol.
We have now provided the fraction of multiply charged aerosol for all the sizes in section 3.1 (see page 5 line 10-21). However, we would like to re-iterate that the fraction of multiply charged particles have no bearing on this statement, as the convergence is occurring at the higher surface areas (i.e. larger particles sizes) where we have the fewest percentage of multiple charged particles (see section 3.1 of revised manuscript).

P7L10-11: I advise not to use T_{50} for comparison to other studies. In this regard, my suggestion from above, i.e., showing $n_s(T)$, would be helpful.
We have included $n_s(T)$ (we use the term INAS density) in the appendix following the Reviewer recommendations. It is not clear from the Reviewer's comment why in addition a comparison using T_{50} cannot be presented.

P7L23-25: "it remains unknown what particle property other than chemistry and crystallography or morphological features … could be active sites": This conclusion cannot be made at this point in the manuscript since you only discuss these factors in Sec. 5. Please reword. On P7L25, do you mean "as discussed"?
Agreed, we have rephrased the statement, which is meant to introduce and explain the structuring of the discussion and not to draw any conclusions (see page 8 line 10-12).

P8L8: "sanidine" should also be followed by a comma.
Done (page 8 line 27)

P8L11: Sometimes you use "(see Figure…)", sometimes only "(Figure…)". Be consistent.
This is not accidental; there is no need for consistency here, because the two indicate different things. When we say "see Figure xx" we are suggesting that a reader should look at the Figure while reading that sentence, and when we just say (Figure xx) we are informing the reader where the relevant information is available.

P8L13-14: What is the difference between a defect-free and an ordered crystal? Please clarify.
The degree of order and disorder in feldspars is determine by the distribution of silicon and aluminum distribution within the tetrahedrons, in sanidine the distribution is random, where as in an ordered crystal (microcline), the distribution of these atoms are regular. Defects can occur in both, ordered or disordered crystals, since a defect would imply a point defect or a line defect. In the former, this can be because of a

vacancy at a point where there should be an atom, or the presence of an atom at a location where there should be empty (interstitial space). Line defects can occur if atoms are misaligned

P8L29: I think, it might be helpful to indicate the perthitic structures in Fig. 6, maybe with the help of overlaid boxes.
We think this could reduce the aesthetic of the images. But we add a description to the caption in Figure 6 and refer to it at the said location now page 9 line 20-23

P9L29: "Contrary to the Pb content, …": Are you referring to microcline not quite fitting the linear relation in Fig. 7? This should be discussed in the previous paragraph.
Done (see page 10 line 15-16 and line 23-24).

P10L4: Move "(increase entropy)" behind "structuring of water".
Done (page 11 line 8)

P10L6-7: The explanations of kosmotropic and chaotropic in brackets should be moved to P10L2, where the terms are first mentioned.
Done (now page 11 line 6)

P10L10-11: I suggest to move this statement towards the beginning of Sec. 5.2. Otherwise the reader might wonder for quite some time how valid your conclusions about the bulk chemical composition are for the investigated submicron particles.
Done. We moved this sentence to page 10 line 9-10 at the beginning of section 5.2. In addition, we also refer to the INAS densities in appendix A to demonstrate the similarity in composition with particle size.

P10L28: Insert comma between "cold" and "low".
Done, (page 12, line 1).

P11L9: Missing bracket after "sanidine".
Done – thanks (page 12 line 14).

P11L25-26: Either change "temperatures" to "a temperature" or "that" to "those".
We restructured this sentence to "above homogeneous freezing temperatures" so that the plural use is more obvious (page 12 line 32)

References:

Augustin-Bauditz, S., Wex, H., Kanter, S., Ebert, M., Niedermeier, D., Stolz, F., Prager, A., and Stratmann, F.: The immersion mode ice nucleation behavior of mineral dusts: A comparison of different pure and surface modified dusts, Geophys. Res. Lett., 41, 7375-7382, doi:10.1002/2014GL061317, 2014.

Harrison, A. D., Whale, T. F., Carpenter, M. A., Holden, M. A., Neve, L., O'Sullivan, D., Vergara Temprado, J., and Murray, B. J.: Not all feldspars are equal: a survey of ice nucleating properties across the feldspar group of minerals, Atmos. Chem. Phys., 16, 10927-10940, doi:10.5194/acp-16-10927-2016, 2016.

Hartmann, S., Wex, H., Clauss, T., Augustin-Bauditz, S., Niedermeier, D., Rösch, M., and Stratmann, F.: Immersion Freezing of Kaolinite: Scaling with Particle Surface Area, J. Atmos. Sci., 73, 263-278, doi:10.1175/JAS-D-15-0057.1, 2016.

Peckhaus, A., Kiselev, A., Hiron, T., Ebert, M., and Leisner, T.: A comparative study of K-rich and Na/Ca-rich feldspar ice-nucleating particles in a nanoliter droplet freezing assay, Atmos. Chem. Phys., 16, 11477-11496, doi:10.5194/acp-16-11477-2016, 2016.

Whale, T. F., Holden, M. A., Kulak, A. N., Kim, Y.-Y., Meldrum, F. C., Christenson, H. K., and Murray, B. J.: The role of phase separation and related topography in the exceptional ice-nucleating ability of alkali feldspars, Phys. Chem. Chem. Phys., 19, 31186-31193, doi:10.1039/C7CP04898J, 2017.

References

Lüönd, F., Stetzer, O., Welti, A., and Lohmann, U.: Experimental study on the ice nucleation ability of size-selected kaolinite particles in the immersion mode, J. Geophys. Res.-Atmos., 115, DOI:10.1029/2009jd012959, 2010.

Reviewer comments have been reproduced in bold and author responses in regular typeface.

Referee report on "Ice nucleation properties of K-feldspar polymorphs and plagioclase feldspars" by André Welti et al. The paper "Ice nucleation properties of K-feldspar polymorphs and plagioclase feldspars" by A. Welti, U. Lohmann, and Z. Kanji continues the series of experimental studies aimed at understanding the ice nucleating (IN) properties of the feldspar component of atmospheric mineral dust (MD). In particular, the role of potassium-rich feldspar and its modifications requires a thorough characterization due to its abundance in the atmosphere and the easiness it triggers ice nucleation in supercooled water or supersaturated water vapor.

Apart from reporting the results of freezing experiments, the manuscript suggests that some qualitative correlations between the feldspar genesis and its IN activity could be established. However, as many factors (pressure, temperature of crystallization, cooling rate, presence of volatile fluxes, shearing stress, variations in bulk composition of magmatic fluid, etc.) can influence the structure of the K-feldspar in igneous rocks, the authors do not attempt specifying a mechanism responsible for the strong variation of IN activity of feldspar. Even so, establishing such correlations could provide a useful tool to predict what kind of feldspar might me expected to be a better IN particle. From this point of view, the correlation between median freezing temperature and Rb/Sr ratio appears to be especially promising (more on that below). I therefore support the publication of the manuscript but would like to attract authors' attention to the following issues:

1. The manuscript reports size resolved immersion freezing experiments on 9 new types of feldspar using a single-particle continuous flow diffusion chamber (CFDC), and thus presents a large body of new data that could be used for parameterization of IN activity of feldspar-containing MD aerosols in cloud models. However, the data is not presented in terms of ice nucleating active site (INAS) density, which became standard for reporting the IN properties of aerosol particles over the past years. Although the possibility of such analysis is indicated (end of section 4.1) and obviously has been conducted for amazonite sample (Ickes et al. 2017), it was not extended to other samples and sizes in this manuscript. This is particularly unfortunate, as the experimental conditions (using mobility-selected single feldspar particles as INPs and well-defined thermodynamic conditions in the CFDC) are ideally suited for performing the INAS density-based analysis. This would substantially simplify the comparison of the results with the numerous data of recent IN experiments on feldspar. I strongly recommend including this analysis into the revised version of the manuscript. Additionally, the size distributions of aerosol particles used in the experiments have to be added to the manuscript (as a supplement) or made available for anyone who would be interested to calculate the INAS densities.

We added the figure below as Appendix A in the revised manuscript showing INAS densities. Compared to the experimental data shown in Fig. 3 of the manuscript, INAS density (n_s) scales the frozen fraction (FF) by the particle surface area according to:

$$n_s = \frac{ln(1 - FF)}{A}$$

Where A denotes the geometric surface area, calculated as $A = 4\pi\left(\frac{\mathrm{d}}{2}\right)^2$, with d being the selected mobility diameter. Because measurements are conducted with quasi monodisperse particles, INAS densities can easily be calculated without the need for individual size distributions.

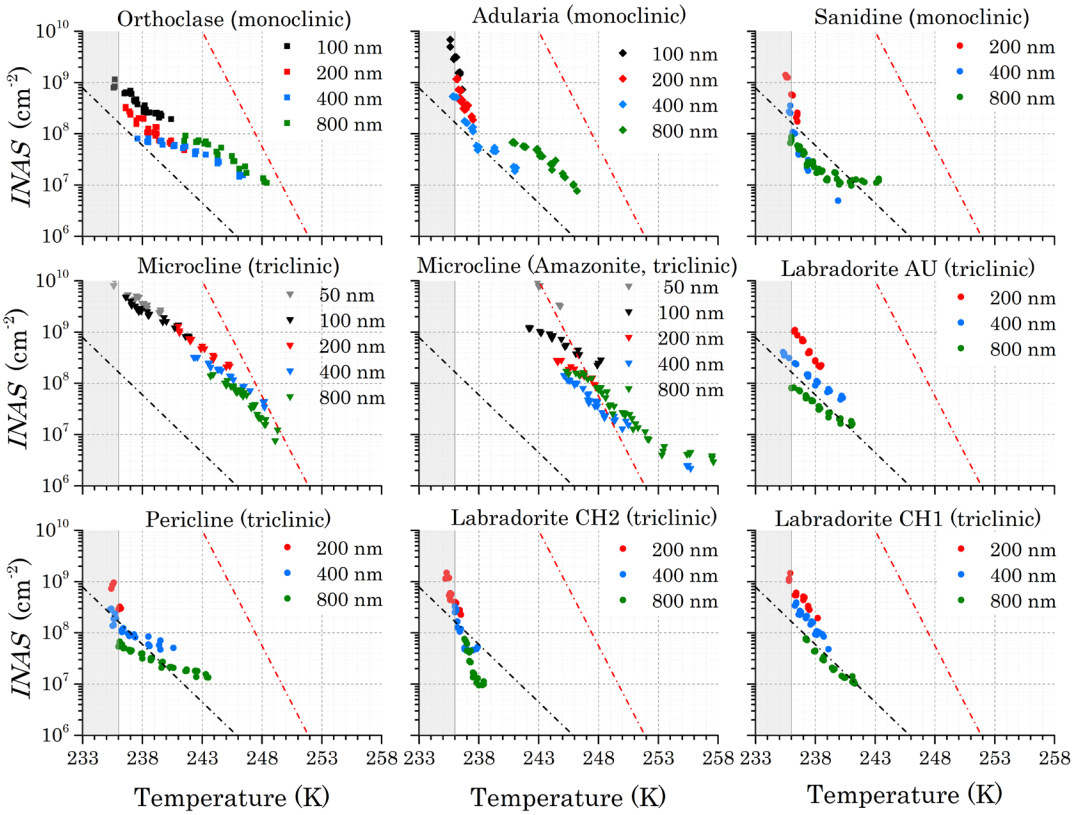

Figure A1 (in revised manuscript): Ice nucleation sites per surface area (INAS) of 9 feldspar samples as a function of temperature and size corresponding to observed frozen fractions as shown in Figure 3. The upper (80-100%) and lower (0-20%) frozen fractions have been omitted to exclude saturation errors from the detection.

2. That the IN properties of all feldspars are size dependent, is convincingly shown by the figure 5. It is also apparent that the T50 values for the smallest particle sizes in each curve lie in the homogeneous freezing range, implying that the T50 values have been calculated for all droplets, frozen both heterogeneously and homogeneously. This doesn't make sense to me. What is the purpose of reporting the median freezing temperature for particles that did not induce freezing of supercooled droplets? Was it not possible to correct the frozen fraction for homogeneously frozen droplets? Again, this is a very strong argument for reporting the INAS densities instead of median freezing temperatures.

In cases when homogeneous and heterogeneous nucleation contribute to ice formation, it is beyond the experimental capacity to accurately determine the corresponding fractions. When the measured T_{50} lies within homogeneous freezing temperatures, all that can be deduced with confidence is that the corresponding sample is not an efficient ice nucleator in the immersion mode at temperatures above homogenous freezing temperature. In response to the Reviewer request, we instead removed the T_{50} data from Figure 5 if a frozen fraction of 50% was not reached above the homogeneous freezing temperature. As requested by the Reviewer, INAS densities have now been included in the appendix (see comment above). It can be seen from these plots that normalizing frozen fractions by the particle surface area in the homogeneous nucleation regime, does not produce overlapping (except for amazonite), but rather

parallel displaced INAS densities. This is an artifact of the *INAS* scaling, treating homogeneous freezing that is not dependent on the size of immersed particles, the same as heterogeneous freezing.

3. Another major (critical) comment is that the reported correlations between crystalline structure, trace element composition, and IN activity are not sufficiently supported by statistics. The authors state that IN efficiency is correlated with the degree of ordering of Si and Al atoms in the feldspar framework, implying that there must be a mechanism responsible for this correlation. This mechanism is not discussed in the manuscript, nor is the suggested correlation expressed in any quantitative manner (although such quantity can be derived, see for example, (Smith 1970, Brown and Parsons 1989). I doubt that such correlation could be of practical use unless a mechanistic explanation is suggested or a quantitative correlation analysis is performed.

In the initial manuscript, we already explain that we cannot give a reason for the correlation of crystal structures and the ice nucleation activity of feldspars, since the crystal structures do not match that of ice. We agree the explanations given in the manuscript are qualitative (not supported by statistics) as pointed out by Reviewer 2. However, in the reference given by the reviewer (Smith, 1970), the author also confirms that in theory a quantitative description of order-disorder of crystal structure is possible but this has not been done quantitatively as it poses additional complexity and challenges. As such even in Brown and Parsons (1989), the second reference suggested by the reviewer, only a qualitative description is suggested. Quantifying the degree of order in feldspar samples would likely be a full study of its own and much beyond the scope of this work.

The intention of discussing crystalline structure and trace elemental composition is to highlight the possibility that several feldspar properties are connected (e.g. by the conditions of rock formation), and more detailed investigations are needed to disentangle their importance for the ice nucleation activity and the mechanism. Because the lack of a mechanistic understanding we prefer not to provide statistical correlations that could be misunderstood as parametrizations and hope this study to serve as a stepping stone for future studies aiming to establish a quantitative understanding.

Nevertheless, we suggest that it is possible to identify properties which can be used as qualitative tracers (not causes) for the ice nucleation activity. Focus is therefore placed on the most practical tracer, which we think is the trace elemental composition, for which qualitative agreement is shown in Figures 7 and 8.

3. With respect to the trace elements composition, the number of investigated samples is definitely too low to draw any particular conclusion. I agree that for the presented choice of samples, the correlation between the IN activity and the ratio of Rb/Sr content is striking. On the other hand, the partitioning of trace elements takes place as feldspar is cooling and forming separate phases, so that Rb replaces K and Sr replaces Ca; thus the Rb/Sr ratio is indicative for the position of feldspar on the ternary phase diagram (An-Ab-Or) and the absolute concentrations of trace elements depends on the cooling/crystallization process and abundance of trace elements in particular magmatic fluid (Parsons et al. 2008). As a consequence, the high Rb content is expected in low microcline and the observed correlation just reflects the correlation between the IN activity and microstructure of feldspar. It is still very interesting that the most IN active sample has also the highest Rb content, an order of magnitude higher than the second-best microcline. I think this fact deserves to be highlighted in the manuscript, even if no mechanistic explanation can be offered at the moment. With the amount of experimental data on IN properties of feldspars that recently became available, it would be relatively easy to improve the statistical analysis and to show if the connection of IN activity and Rb content is not just a coincidence. I would really like to see such analysis in the manuscript or in the follow-up work.

We fully agree with the reviewer that we should highlight better that a replacement of K by Rb results in a lower microcline polymorph, yet a higher Rb/Sr ratio, thus a higher ice nucleation activity suggesting that observed correlation reflects a potential relationship between ice nucleation activity and feldspar microstructure. We also agree, with more samples than those used here, a systematic analysis of available data in light of the findings in this manuscript could be a promising follow-up study. Following the Reviewer recommendation, we added:

Page 10 line 31-page 11 line 3:"The Rb/Sr ratio is indicative for the position of feldspar on the ternary phase diagram (Figure 1) and the absolute concentrations of trace elements depends on the cooling/crystallization process and abundance of trace elements in particular magmatic fluid (Parsons et al., 2009). The replacement of K by Rb results in a lower microcline polymorph, and a higher Rb/Sr ratio, correlating to higher ice nucleation activity. This suggests that the observed correlation reflects a possible relationship between ice nucleation activity and feldspar microstructure."

Page 12, line 20-23: "More ice nucleation active samples show higher Rb/Sr ratios, e.g., the most active microcline sample has an order of magnitude higher Rb/Sr ratio than the second-best microcline. Therefore, Rb/Sr ratios could serve as tracer for highly ice nucleation active feldspar particles or even help to differentiate sources of feldspars acting as INP at specific temperatures."

4. I am also confused by the discussion of Pb content and its correlation with the median freezing temperature. The authors state that "The best linear correlation between a single compound and the ice nucleation activity based on T50, was found for the Pb content in the feldspar samples (Figure 7).", but obviously the Pb content in microcline (better IN) is lower than in orthoclase (weaker IN). The quality of the correlation as expressed by Pearson's r-coefficient is apparently influenced by the low Pb content in the plagioclase and high-temperature disordered alkali feldspar, which has been formed before any trace elements partitioning could take place. I think the plagioclase feldspars should be excluded from the correlation analysis. If you do that, the correlation between T50 and Rb/Sr content ratio would be even better than for Pb and the T50 as a function of Rb/Sr would be also monotonically rising.

On a side note, if Pb is normalized by Nd content, the correlation between T50 and Pb/Nd ratio becomes very clear, with T50 as a function of Pb/Nd staying constant for plagioclases and then monotonically rising from the level of adularia and sanidine towards amazonite. This is just to illustrate that such correlations can be constructed very easily and most of them are probably meaningless, unless a larger set of samples is analyzed or an underlying physical and chemical mechanism is suggested. I encourage the authors to do so.

The decision to compare T_{50} to Pb, Rb and Sr is based on the random forest analysis which identified these three as the most promising predictors. The *r*-coefficients in the text, give the correlation between these elements and not to the T_{50} as the Reviewer states, as such we will clarify the statement so that a potential reader does not mis-understand the correlation. Furthermore, we share the view of the Reviewer that the correlation of Pb content and T_{50} is biased by the low content in the plagioclase feldspars, the limited number of samples and potential sub sequential uptake. It is because of Pb is suggested by the random forest analysis that we discuss it and then argue to discard it as a predictor. We thank the Reviewer for pointing out the possibility to create a monotonic correlation between T_{50} and Pb/Nd. However, in contrast to Rb/Sr, we did not find any literature suggesting an interpretation of this ratio.

To clarify we now write:
Page 10, line 24-25 "Based on these arguments and that the correlation of Pb content to T_{50} is not monotonic (e.g., lower Pb content in microcline than orthoclase, Figure 7) we focus on other predictors suggested by the Random Forest analysis.

Page 11 line 3-5: "We note that a monotonic correlation between T_{50} and a Pb/Nd ratio can also be constructed, but no interpretation of the implication of such a ratio could be found in the literature and neither was Nd suggested as a predictor by the Random Forest analysis."

5. With respect to the potential predictability of IN activity based on the relative concentrations of trace elements, I have to point out that the measurements reported here have been conducted exclusively with the single-crystal samples. In case of real-world atmospheric mineral dust, the majority of feldspar would be coming from phenocrysts (inclusions of feldspar in e.g. granite matrix), where the trace elements content could be very different. Again, the idea of using partitioning of trace elements as a predictor for IN efficacy is very attractive and promising, but must be explored deeper and supported by extensive dataset.

We already discuss this limitation of the study in regard to atmospheric aging in the initial manuscript page 10 lines 20-24 (page 11 lines 26-30 in revised manuscript) but we clarify this further prompted by the Reviewer comment and added the following to the revised manuscript:

Page 11, line 31-32: **"**Additionally, a majority of airborne feldspar particles could be coming from phenocrysts (inclusions of feldspar in e.g. granite matrix), where the trace element content could be different."

Specific remarks (ordered according to page and line number, citations given in italic):
1-14. The sentence "Ice nucleation is most efficient on the crystallographic ordered, triclinic K-feldspar species microcline, while the intermediate and disordered, monoclinic K-feldspar polymorphs orthoclase and sanidine nucleate ice at lower temperatures." strongly implies a causality between the degree of ordering and IN efficacy. Since such causality is not supported by the experimental data of the manuscript, I suggest that the sentence should be reformulated.

We agree with the Reviewer and in order to limit the statement we now write (Page 1 line 14):
"Amongst the investigated samples, ice nucleation is most efficient on the crystallographic ordered, triclinic K-feldspar species microcline, while the intermediate and disordered, monoclinic K-feldspar polymorphs orthoclase and sanidine nucleate ice at lower temperatures."

1-26 (Introduction). The introduction would greatly benefit from including a discussion of partitioning of the trace elements in feldspars. As mentioned above, the possible correlation between trace elements and IN activity can open a unique opportunity to classify the feldspars on a single-particle basis, for example in a laser ablation mass spectrometer.

We think it would be premature to discuss the partitioning of specific trace elements in the introduction, as the correlation of the trace elements to the ice nucleation activity is shown as a result of the current study. However, prompted by the Reviewer's suggestion, we do include a paragraph on trace elements and their importance to feldspar microtexture and characteristics, in the introduction (see page 3 lines 19-27). Additionally, we have added discussions on partitioning of the trace elements in the following places: Page 10 lines 32 to page 11 line 5 and Page 12 lines 20=23.

2-9. The degree of order (or disorder) of Al3+ and Si4+ is not something that an average atmospheric scientist would be familiar with. This sentence requires explanation.

We elaborate further on this topic on page 2 line 14-15:
"The four units are made up of one Al^{3+} and three Si^{4+} ions. In a disordered state Al^{3+} can be found in any one of the four tetrahedral sites while in an ordered state Al^{3+} occupies the same site throughout the crystal (Nesse, 2016)."

3-2. (Whale et al. 2017) did not conduct systematic study of crystalline structure in terms of disorder, although they report the fraction of orthoclase in their perthitic samples. A careful analysis of their samples could have reveal a correlation. Please elaborate on that issue.

Whale et al. 2017 do discuss order-disorder in their article. In the supplementary material they give a comprehensive summary on the order-disorder of K-feldspar and they have measured it by Raman spectroscopy for some of their samples. It is mentioned that it has been under discussion in relation to ice nucleation ability in other studies. By pointing to examples where disordered feldspar samples showed high ice nucleation activity when measured with their setup they conclude that it is not a necessary feature. However, different from the current study, their experimental setup is sensitive to much rarer particle features (ice active at much higher temperatures) than a single particle investigation, thus the conclusions might not be transferrable.

3-14. (Niedermeier et al. 2015) has reported nucleation ability of size-resolved K-feldspar sample in single-particle immersion mode and according to the manuscript, the microcline data from your study has been previously published in (Ickes et al. 2017). So the statement "for the first time" must be either removed or explained, what exactly has been done in this work for the first time.

We removed the statement (Page 3 line 29).

3-21 (Section 2). A more detailed description of the sample origin and the XRF analysis would be very helpful here. Was XRF analysis the only basis for identifying the samples or have you performed the powder XRD analysis, too? Could you speculate on how the chemical composition of single aerosol particles would be related to the chemical composition measured for bulk samples?

Composition of the samples were additionally determined by Rietveld refinement of powder XRD pattern. Note that this method is subjective to the fitting procedure to some degree. Results are given below and have been added as Appendix B in in the manuscript.

Sample	orthoclase	adularia	sanidine	microcline	plagioclase	quartz	Others
Orthoclase	70				15	5	10
Adularia		100					
Sanidine			100				
Microcline				90	10		
Microcline (Amazonite)				77	22	1	
Labradorite (AU)					59	12	29
Pericline					84	16	
Labradorite CH2					100		
Labradorite CH1					100		

Samples were provided from the geological collection of ETH Zürich except Labradorite (AU) which is a commercial sample sold in powder form as supplement for ceramics and Amazonite which was provided by a private collector. Because for all except Labradorite (AU), fine particles are obtained by grinding single stones, we expect the bulk chemical analysis to be a good approximation for the majority of particles. However, this was not investigated experimentally and certain compounds may be more abundant at a certain particle size.

3-27. The sample that is called "orthoclase" here should be the one closest to the ideal end-member of the alkali feldspar group (Or = KAlSi3O8). On the Figure 1, however, this sample has the same composition as amazonite with almost 20% albite. Where the name "orthoclase" came from? By the way, it is not correct to label the axes of the ternary phase diagram with fraction of K, Na, or Ca. The ternary diagram gives a sample composition in terms of weight fractions of end-members (orthoclase, albite, and anorthite), see for example (Parsons 2010). The name orthoclase is also misspelled in the legend. Please correct.

The sample was identified as orthoclase by experts and subsequent analysis (see table B1 in revised manuscript) confirmed orthoclase as the primary component. Lacking a more correct alternative, we kept the name. We have in addition added the end member names to the ternary phase diagram. We have kept the axis with fraction of K, Ca and Na since we used this analysis from the XRF to place the samples onto the ternary phase diagram as mentioned in the caption of Figure 1 already in the initial manuscript. We corrected the spelling and Figure 1 accordingly.

4-3. Table 3: What is the purpose of reporting compounds that could not be detected in any of the samples (FeO, NiO, H2O, CO2)? What is the difference between a "0" and N/D?

The respective compounds have been removed. "0" indicates a reliable measurement of absence of a compound, while N/D stands for not detected.

6-21:22. This kind of analysis has been published even before (Ickes et al. 2017) and should be mentioned here. See, for example (Wright et al. 2013, Niedermeier et al. 2015, Peckhaus et al. 2016) to name just a few.

We added to Page 7 line 9-10: "Parametrizations for other feldspar samples can be found in e.g., Niedermeier et al., 2015; Peckhaus et al., 2016"
Wright et al., 2013 did not report a feldspar parametrization.

7 (Section 4.2) This section should be expanded to include more thorough size dependence analysis, ideally complimented by the INAS density calculations. The T50 should be corrected to account for the homogeneous freezing of droplets containing the smallest particle sizes. Some specific question here: why would one expect linear dependence of T50? The median freezing temperature is a function of cooling rate and residence time, have you taken this into account when comparing T50 from your measurements and data from Atkinson et al., (2013)? 7-9. "The minimum size triggering immersion freezing is found to be 50 nm microcline particles". In the Sample preparation section you mention that a "substantial fraction of larger multiple charged particles… among the 50nm particles can be expected". How substantial is this fraction? Since the frozen fraction ends in the homogeneous freezing regime at 0.3 (Figure 3), is there a way to decide if the 50 nm microcline particles have been responsible for freezing at all or only the multiply charged larger particles are responsible? On the other hand, the

freezing curve for 50 nm amazonite particles reaches value of 0.9 suggesting that all particles have been active. Could that be that even smaller particles would be IN active?

A figure showing the calculated *INAS* density has been included in the appendix. Data points where homogenous freezing strongly contributes to the 50% frozen fraction have been deleted from Figure 5.

A linear dependence of T_{50} in a lin-log plot is expected for CNT based parametrizations using single contact angle or a log-normal contact angle distribution (Welti et al., 2012, Fig. 10).

We did not apply a correction for time dependence when comparing to Atkinson et al., 2013. This is not necessary as both the residence time in the current experiment (12s) and the cooling rate in the Atkinson et al., 2013 experiment (1K/min) maintain the sample at the reported temperature for a comparable duration, i.e. experimental uncertainties outweigh time dependence.

The multiple charged fraction of selected 50nm, amounts to 30% doubly charged, 73nm and 7% triple charged, 91nm particles, while 63% of particles are 50nm. . Based on the size dependence of immersion freezing and the abundance of multiple charged particles, the contribution of the 3 particle sizes at different frozen fractions can be calculated. The result is shown in the Figure below (and now shown and explained in the revised manuscript Appendix C).

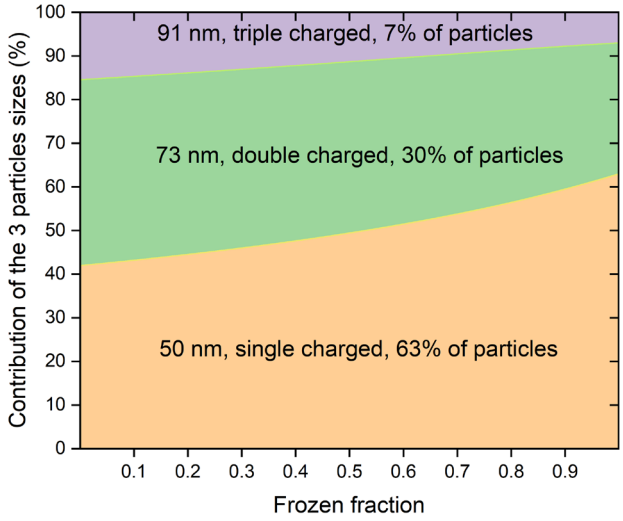

We now clarify this aspect on page 5 line 21 and page 8 line 4-5.

50nm particles contribute more than 40% of ice active particles at any frozen fraction. Based on the current measurements it seems plausible that for some microcline species, particles smaller than 50nm are ice active. But it is difficult to produce such small particles.

8-25 Twinning is not just symmetrical intergrowth. In alkali feldspars twinning is interrelated with phase exsolution and Na-K exchange between phases or between feldspar and external aqueous fluids (Parsons et al. 2015).

The section was changed accordingly and the reference was added (see page 9 line 14-16 in the revised manuscript).

9-4. How thick was the Pt coating applied prior to SEM imaging? For the confinement effects to become

important the pores should be less than 10 nm in diameter, could you reach this resolution in the SEM analysis?

Sputtered films for SEM typically have a thickness range of 2–20 nm. The resolution of the SEM is 1 -1.7 nm. As no pores are detected in the SEM images, and smaller pores that could have been missed in the SEM analysis and are small enough to supress ice formation, we conclude that using the geometric surface is a better measure for the particle surface area than the BET-surface.

9-9. "The assumption that physical properties (e.g. hardness) are comparable among the tested feldspar species implies that the same degree of artificial surface features are introduced to all samples." What is the background for such assumption? Could you support it by literature data? On the page 3 line 32 I read something different: "The different polymorphs differ in physical properties (cleavage, hardness, specific weight, melting point)…" Could you clarify this point?

Feldspar do have very similar properties. As an example, their hardness is typically between 6 - 6.5 on Mohrs scale. https://en.wikipedia.org/wiki/Feldspar

We changed the sentence p.3, line 32 (now page 4 line 14) to "The different polymorphs differ in some physical properties (e.g. melting point) and are found in different rocks:…"

10-5. The discussion of kosmotropic vs. chaotropic cations is not very convincing. Why would the substitution of K+ for Rb+ increase the IN efficiency of K-rich feldspar if K+ is already kosmotropic? Or is there anything known about the degree of "kosmotropicity" for different kosmotropic cations? How many ions of Rb+ would one expect on the surface of an aerosol particle? Why some Na/Ca-rich feldspars exhibit a strong IN activity, having neither K+ nor Rb+ in their structure (like amelia albite in Whale et al., 2017)? This hypothesis should be either discussed in more detail or just omitted from the manuscript.

We clarify this discussion as suggested by the reviewer, but keep it in the manuscript as a possible second explanation, for the observed correlation between Rb/Sr and the ice nucleation activity of the feldspars (page 11 lines 3-13). To relativize the importance we added (page 11 line 13-15): "It would be necessary to quantify the concentration of cations required to influence water ordering to determine how influential Rb^{+} and Sr^{2+} are for ice nucleation given their trace elemental composition.

I am looking forward to the revised version of the manuscript.

References

1. Brown, W. L. and I. Parsons (1989). "Alkali feldspars: ordering rates, phase transformations and behaviour diagrams for igneous rocks." Mineralogical Magazine 53(369): 25-42 doi:10.1180/minmag.1989.053.369.03.

2. Ickes, L., A. Welti and U. Lohmann (2017). "Classical nucleation theory of immersion freezing: sensitivity of contact angle schemes to thermodynamic and kinetic parameters." Atmos. Chem. Phys. 17(3): 1713-1739 doi: 10.5194/acp-17-1713-2017.

3. Niedermeier, D., S. Augustin-Bauditz, S. Hartmann, H. Wex, K. Ignatius and F. Stratmann (2015). "Can we define an asymptotic value for the ice active surface site density for heterogeneous ice nucleation?" Journal of Geophysical Research: Atmospheres: n/a-n/a doi: 10.1002/2014jd022814.

4. Parsons, I. (2010). Feldspars defined and described: a pair of posters published by the Mineralogical Society. Sources and supporting information. Mineralogical Magazine. 74: 529.

5. Parsons, I., J. D. Fitz Gerald and M. R. Lee (2015). "Routine characterization and interpretation of complex alkali feldspar intergrowths." American Mineralogist 100(5-6): 1277-1303 doi: 10.2138/am-2015-5094.

6. Parsons, I., C. W. Magee, C. M. Allen, J. M. G. Shelley and M. R. Lee (2008). "Mutual replacement reactions in alkali feldspars II: trace element partitioning and geothermometry." Contributions to Mineralogy and Petrology 157(5): 663 doi: 10.1007/s00410-008-0358-1.

7. Peckhaus, A., A. Kiselev, T. Hiron, M. Ebert and T. Leisner (2016). "A comparative study of K-rich and Na/Ca-rich feldspar ice-nucleating particles in a nanoliter droplet freezing assay." Atmos. Chem. Phys. 16(18): 11477-11496 doi: 10.5194/acp-16-11477-2016.

8. Smith, J. V. (1970). "Physical properties of order-disorder structures with especial reference to feldspar minerals." Lithos 3(2): 145-160 doi: https://doi.org/10.1016/0024-4937(70)90070-8.

9. Whale, T. F., M. A. Holden, A. N. Kulak, Y.-Y. Kim, F. C. Meldrum, H. K. Christenson and B. J. Murray (2017). "The role of phase separation and related topography in the exceptional ice-nucleating ability of alkali feldspars." Physical Chemistry Chemical Physics 19(46): 31186-31193 doi: 10.1039/C7CP04898J.

10. Wright, T. P., M. D. Petters, J. D. Hader, T. Morton and A. L. Holder (2013). "Minimal cooling rate dependence of ice nuclei activity in the immersion mode." Journal of Geophysical Research: Atmospheres 118(18): 10,510-535,543 doi: 10.1002/jgrd.50810.

References

Brown, W. L., and Parsons, I.: ALKALI FELDSPARS - ORDERING RATES, PHASE-TRANSFORMATIONS AND BEHAVIOR DIAGRAMS FOR IGNEOUS ROCKS, Mineral. Mag., 53, 25-42, doi:10.1180/minmag.1989.053.369.03, 1989.

Nesse, W. D.: Introduction to Mineralogy 3rd ed., Oxford University Press, 2016.

Parsons, I., Magee, C. W., Allen, C. M., Shelley, J. M. G., and Lee, M. R.: Mutual replacement reactions in alkali feldspars II: trace element partitioning and geothermometry, Contrib. Mineral. Petrol., 157, 663-687, doi:10.1007/s00410-008-0358-1, 2009.

Smith, J. V.: Physical properties of order-disorder structures with especial reference to feldspar minerals, Lithos, 3, 145-160, doi:https://doi.org/10.1016/0024-4937(70)90070-8, 1970.

Welti, A., Lüönd, F., Kanji, Z. A., Stetzer, O., and Lohmann, U.: Time dependence of immersion freezing: an experimental study on size selected kaolinite particles, Atmos. Chem. Phys., 12, 9893-9907, doi:10.5194/acp-12-9893-2012, 2012.

Ice nucleation properties of K-feldspar polymorphs and plagioclase feldspars

André Welti[1,2], Ulrike Lohmann[1] and Zamin A. Kanji[1]

[1]ETH Zurich, Institute for Atmospheric and Climate Science, Zurich, 8092, Switzerland
[2]now at: Finnish Meteorological Institute, Helsinki, FI-00101, Finland

Correspondence to: Zamin A. Kanji (zamin.kanji@env.ethz.ch)

Abstract. The relation between the mineralogical characteristics of size selected feldspar particles from 50 – 800 nm and their ability to act as ice nucleating particles (INPs) in the immersion mode is presented. Five polymorph members of K-feldspar (two microclines, orthoclase, adularia and sanidine) and four plagioclase samples (three labradorites and a pericline sample) are tested. Microcline was found to be the most active INP in the immersion mode consistent with previous findings. Samples were selected for their differences in typical feldspar properties such as crystal structure, bulk and trace elemental composition and ordering of the crystal lattice. The mentioned properties are related to the temperature of feldspar crystallization from the magma during formation. Properties characteristic for low temperature feldspar formation coincide with an increased ability to nucleate ice. Amongst the samples investigated, ice nucleation is most efficient on the crystallographic ordered, triclinic K-feldspar species microcline, while the intermediate and disordered, monoclinic K-feldspar polymorphs orthoclase and sanidine nucleate ice at lower temperatures. The ice nucleation ability of disordered, triclinic Na/Ca-feldspar is comparable to disordered K-feldspar. The conditions of feldspar rock formation also leave a chemical fingerprint with varying abundance of trace elements in the samples. X-ray fluorescence spectroscopy analysis was conducted to determine metal oxide and trace elemental composition of the feldspar samples. The analysis revealed a correlation of trace metal abundance with median freezing temperatures (T_{50}) of the K-feldspar samples allowing to sort them for their ice nucleation efficiency according to the abundance of specific trace elements. A pronounced size dependence of ice nucleation activity for the feldspar samples is observed, with the activity of smaller sized particles scaling with surface area or being even higher compared to larger particles. The size dependence varies for different feldspar samples. In particular, microcline exhibited immersion freezing even for 50 nm particles which is unique for heterogeneous ice nucleation of mineral dusts. This suggests that small microcline particles that are susceptible to long-range transport can affect cloud properties via immersion freezing far away from the source. The measurements generally imply that temperatures at which feldspars can affect cloud glaciation depend on the transported particle size in addition to the abundance of these particles.

Deleted: Na/Ca- rich feldspar

Deleted: are

Deleted: melt rocks

Deleted: I

Deleted:

Deleted: A pronounced size dependence of ice nucleation activity for the feldspar samples is observed, which also depends on mineralogical characteristics.

Deleted: s

Deleted: and

Deleted: .

1. Introduction

Freezing of water droplets in supercooled clouds begins in a number of ways. Cloud droplets with a typical mean diameter of 10 µm freeze by homogeneous nucleation at temperatures below 235 K. Above homogeneous nucleation temperatures, drop freezing is initiated through heterogeneous ice nucleation by inclusions in water droplets (immersion freezing), serving as substrates for ice nucleation or by particle collisions with cloud droplets (contact freezing). Dependent on the type of particle, the probability that heterogeneous ice nucleation occurs at a certain temperature differs. Through the analysis of ice crystal residuals it was discovered, that often mineral dust particles serve as ice nucleation substrates (e.g., Kumai, 1951). Rosinski (1979) identified feldspar (orthoclase) as one of the mineral residuals. Feldspar is the most abundant mineral type in the outer crust of the earth (Lutgens et al., 2014) and therefore a common compound of desert dusts and volcanic ejecta (Knippertz and Stuut, 2014). The feldspar minerals can be grouped according to bulk composition into potassium rich feldspar (K-feldspar) and Na-, Ca-rich species (plagioclase). While the series of plagioclase contains all fractions of Na, Ca, there is a mixing gap for K-feldspar. Only a limited fraction of K^+ can be replaced by Na^+ or Ca^{2+}. K-feldspar is subdivided into three polymorphs (microcline, orthoclase, sanidine), based upon the degree of order-disorder of Al^{3+} and Si^{4+} in the tetrahedral units forming their crystal network. The units are made up by of one Al^{3+} and three Si^{4+} ions. In a disordered state Al^{3+} can be found in any one of the four tetrahedral sites while in an ordered state Al^{3+} occupies the same site throughout the crystal (Nesse, 2016). Early investigations on the ice nucleation efficiencies of various mineral dust species, including feldspar (orthoclase and microcline) by, e.g. Pruppacher and Sänger (1955); Mason and Maybank (1958); Isono and Ikebe (1960), grouped orthoclase into the less efficient ice nucleating particles compared to mineral species, e.g. muscovite or kaolinite. In addition, differences in ice nucleation between K-feldspar species are already recognized, e.g., Mason and Maybank (1958) reported microcline to have an 8.5 K higher ice nucleating threshold temperature than orthoclase. More recent studies (Zimmermann et al., 2008; Atkinson et al., 2013; Yakobi-Hancock et al., 2013; Harrison et al., 2016; Kaufmann et al., 2016; Kiselev et al., 2016; Peckhaus et al., 2016; Pedevilla et al., 2016; Whale et al., 2017) confirmed that different members of the feldspar group exhibit variable ice nucleation activities in the immersion and deposition mode. Especially samples of microcline were found to be active INPs at higher temperatures than other minerals. Even though feldspar was recognized as an INP in earlier studies, little attention was given to feldspar in the context of atmospheric ice formation. Instead, ice nucleation research focused on clay minerals, probably because feldspar is mainly found in the coarse size fraction in airborne desert dusts (Engelbrecht and Derbyshire, 2010), making it less susceptible to long range transport. In support of this, using X-ray diffraction analysis, Boose et al. (2016) found the feldspar mass fraction in airborne transported dusts to be significantly lower than in surface sampled dusts. Despite the lower mass fraction of feldspars found in the airborne Saharan dust samples, Boose et al. (2016) concluded that these could be relevant for atmospheric cloud glaciation at warmer temperatures (T > 250 K). Explosive volcanic eruptions can introduce large quantities of feldspar particles into the atmosphere with a regional to global effect on cloud glaciation (Mangan et al., 2017). The analysis of ash particles that make up volcanic ash clouds showed that up to 70% can be feldspar (usually plagioclase feldspars, rarely sanidine) particles (Bayhurst et al., 1994,; Schumann et al., 2011).

Deleted: two possible

Deleted: particle inclusions in collisions with cloud droplets (contact freezing) or

Deleted: the

Deleted: immersed in a water droplet,

Deleted: four

Deleted: occupied

Deleted: by

Deleted: units

Deleted: unit

Field Code Changed

Deleted: ¶

Deleted: as

Deleted: and

Deleted: for example,

Deleted: a

Deleted: effectiveness

Deleted: in nucleating ice

Deleted: x

Deleted: ¶

Reasons for why microcline feldspars are active INPs have been discussed in recent studies. A survey of 15 feldspars by Harrison et al. (2016) confirmed the general notion that K-feldspar suspensions show higher freezing temperatures than plagioclase feldspars. In addition to one specific K-feldspar sample being very active with a freezing onset of ~ -2 °C (for 1 wt% suspension) in the immersion mode, Harrison et al. (2016) showed that one sample of a Na-feldspar (Amelia albite), was also particularly ice active exhibiting freezing onset already at -4 °C (for 1 wt% suspension). They also concluded that not all feldspars are equal for their ice nucleation properties even if they are from the same subgroup. Whale et al. (2017) investigated 15 additional alkali feldspars but found no correlation of their ice nucleation activities with their crystal structures or chemical compositions. Instead, they explored specific topographic features on samples that showed exceptionally high ice nucleation temperatures and found that these samples exhibited certain microtexture (perthitic samples) related to phase separation into Na- and K-rich regions whereas samples active at lower temperatures were non-perthitic (Whale et al., 2017). Based on results of a molecular model, Pedevilla et al. (2016) show that freshly cleaved microcline (001 surface) can adsorb a monolayer of water possessing a non-ice like structure, however, overlaying second and third layers will have ice like structures, thus promoting ice nucleation. Kiselev et al. (2016) observed under an electron microscope that even along the perfectly cleaved (001) surface of K-feldspar, ice nucleation occurred on microscopic sites which expose the high-energy (100) surface. This observation was supported by the alignment of growing ice crystals with the (100) surface, regardless of the orientation of the surface (001 or 010) on which ice nucleation occurred. Additionally, ice nucleation predominantly occurred at sites exhibiting steps, crevices or cracks where the high-energy (100) surface is thought to be exposed.

Feldspars contain a variety of trace elements which can, e.g. influence the appearance/colouring of the rock. Some trace elements in feldspars are representative of partitioning during the mineralization process when the rocks form from the parent magma. Microtextures found within feldspar strongly influence the subsequent behaviour of feldspars for example during low temperature weathering and are central to the exchange (or retention) of trace elements (Parsons et al., 2015). Partitioning of trace elements can reveal microtextures, which are related to the distribution of trace elements and point defects that are otherwise difficult to detect in feldspars. Both microtextures and point defects have been suggested to be important for immersion ice nucleation on feldspar polymorphs (Whale et al., 2017). Due to the interlink of feldspar characteristics and trace elemental composition, it may be possible to relate the ice nucleation activity to the concentration of such trace elements within a sample.

In the current study, we present the ice nucleation ability of single immersed, size-selected particles of five K-feldspar polymorphs (see Table 1) with both monoclinic and triclinic crystal structures. Measurements with single immersed particles, allows to explore the lower range of ice nucleation temperatures (< 253 K) within the K-feldspar group, and specially focusing on the effect of particle size. Four Na- and/or Ca-feldspar species are included (see Table 1) to use the feldspar group as a natural system to examine the importance of potential ice nucleating properties (compositional and mineralogical) which slightly vary among its members.

Deleted: can also be composed

Deleted: of

Moved down [2]: Given the numerous trace elements present in feldspar polymorphs, it may be possible to relate the observed ice nucleation activity to the concentration of such trace elements within the sample.

Deleted: at low temperatures

Deleted: is thought to be important because and it

Deleted: are thought

Moved (insertion) [2]

Deleted: Given the numerous trace elements present in feldspar polymorphs

Deleted: observed

Deleted: the

Deleted: for the first time,

Deleted: the

Deleted: ing

2 Sample description

Figure 1 shows a ternary phase diagram of the feldspar samples used in this study. The samples are grouped according to their proportional bulk K-, Ca- and Na- content found by X-ray fluorescence (WD-XRF, Axios, PANalytical). Where known, the samples are named following the mineralogical nomenclature and specific variety, e.g. adularia is a variety of orthoclase and amazonite a variety of microcline. Sample origin, name, mineralogical classification (K-feldspar or Na/Ca-feldspar) and crystal structure are summarized in Table 1. Naming of the plagioclase samples is based on the compositional analysis. For the plagioclase group we have three labradorite samples with different Ca/Na proportions (and the same origin, Switzerland, CH1 and CH2) or the same Ca/Na proportions but different origin (CH2 and Austria, AU), and one form of albite, called pericline (see Table 1). Five K-feldspar samples are investigated including the polymorphs microcline, orthoclase and sanidine. Order-disorder polymorphism occurs due to the effect of pressure, temperature, cooling rate and variations in bulk composition on the ordering process of atoms in the crystalline lattice during petrogenesis i.e. formation of the mineral by crystallization from the melt (Parsons and Boyd, 1971). The lowest ordered polymorph, sanidine, forms at high temperature, orthoclase at intermediate temperature and microcline is the stable polymorph formed at the lowest crystallization temperature. The different polymorphs differ in some physical properties (e.g., melting point) and are found in different rocks: sanidine in volcanic and very high-temperature metamorphic rocks, orthoclase in volcanic and high-temperature metamorphic rocks and microcline in granitic and metamorphic rocks (Lutgens et al., 2014). Depending on the source region, feldspars vary in secondary chemical and trace elemental composition (see Section 5.2). Samples used in this study are not chosen for atmospheric relevance, but to investigate the single particle ice nucleation properties of feldspar particles of different geological origin and interlinked, crystal structure, bulk and trace elemental composition. As such, some samples studied here like adularia and pericline are rare because they typically come from mineral veins and may not be found as the main constituent of airborne dusts (Lee et al., 1998). Similarly, sanidine would also be less abundant in dusts, except following volcanic ash eruptions. However, orthoclase and microcline samples that originate from granites and gneisses do eventually reach the atmosphere after several cycles of weathering and sedimentation (Lee et al., 1998). Plagioclases such as labradorites are common in basalts and as such can be found in volcanic ash from basaltic eruptions (Lee et al., 1998).

3. Experimental Method

All feldspar samples were tested for their ice nucleating ability in the immersion mode by immersing single, size selected particles of mobility diameters between 50 - 800 nm in water droplets. Figure 2 depicts a schematic of the monodisperse particle generation unit and the ice nucleation experiment. The two stages of the experiment are described below.

3.1. Sample preparation

Basic raw materials are single feldspar crystals (adularia, amazonite), one ground sample for use in pottery (labradorite AU) and rocks (all the others). All raw samples are ground for 5 min in a tungsten carbide disc mill (Retsch, RS1, 1400 rpm). The

Deleted: ,

Deleted: s

Deleted: cleavage, hardnes

Deleted: s, specific weight,

Deleted: (

Deleted:)

Deleted: (

Deleted:),

Deleted: (

Deleted:)

Deleted: Table 3)

Moved (insertion) [1]

Deleted: We

Deleted: note that

Moved up [1]: Samples used in this study are not chosen for atmospheric relevance, but to investigate the single particle ice nucleation properties of feldspar particles of different geological origin and interlinked, crystal structure, bulk and trace elemental composition.

Deleted: are

ground sample is aerosolized in a Fluidized Bed Aerosol Generator (TSI Model 3400A). To investigate particle size effects special attention is given to select monodisperse particles. The aerosol is passed through two cyclones (d_{50} =3 µm and 1 µm) and one impactor (d_{50} =0.4 µm) before size selection by a Differential Mobility Analyser (DMA, TSI Model 3081). As the size selection with a DMA is not directly based on the particle size, but on electrostatic mobility, multiple charged particles of larger sizes pass the DMA and are selected as well. Depending on the initial particle size distribution, the fraction of multiple charged particles can contribute a substantial fraction to a certain mobility diameter. In particular, small particle sizes originating from the up-slope of the initial size distribution contain non-negligible amounts of multiple charged, larger particles. To reduce distortion to the size selection, a Centrifugal Particle Mass Analyzer (CPMA, Cambustion), able to isolate a specific particle mass, is used in sequence with the DMA for particle sizes of 100 nm and 200 nm. Spherical particle shape and bulk density (2.6 g cm^{-3}) was assumed to select single charged particles and exclude larger particles by mass. The use of the CPMA for the selection of larger particles (400 nm, 800 nm) was not necessary as the fraction of larger particles is sufficiently reduced by the cyclones and the impactor upstream of the DMA (see Figure 2) which confines the size distribution of the particles entering the DMA to d_{50} = 1 µm (aerodynamic diameter). For the 400 nm size selection, double and triple charged particles (700 and 994 nm) amounted to 16% and 4% respectively, whereas for the 800 nm particles, the doubly charged particles (1481 nm) made up 4%. The CPMA was not used for the selection of 50 nm particles due to the very low number concentration of this particle size in the output size distribution of the fluidized bed generator. A substantial fraction of larger, multiple charged particles (73 nm (~30%), 91 nm (~7%) for 2 and 3 charges, respectively) among the 50 nm (~63%) particles is expected. The contributions of single and multiply charged particles to the frozen fractions is approximately proportional to their abundance and does not impact any of the conclusions made in this work. As all feldspar samples have similar hardness and were ground in the same way, the fraction of multiple charged particles at a selected size is expected to be comparable among samples. The contribution of multiply charged particles to the 50 nm particle frozen fraction is shown in Appendix C.

Deleted: .

Deleted: The resulting removal of large particles from the initial size distribution reduced the contribution from multiple charged particles to the selected aerosol size of 400 and 800 nm.

Deleted: the

Deleted: experiments

Deleted: where as

Deleted: of the particles

Deleted: The multiply charged particles would contribute to the first 10-20% of the frozen fractions reported in this work, but will not impact any of the conclusions made in this work.

Deleted: 4

Deleted: 3

Deleted: can be

Deleted: .

3.2. Immersion Freezing Experiment

A flow of 1 l min^{-1} of sample air containing the dry feldspar particles layered between twice 2.5 l min^{-1} sheath air is introduced into the Immersion Mode Cooling chamber (IMCA) developed by Lüönd et al. (2010). The IMCA walls are 0.6 cm apart and layered with continuously wetted filter paper. A horizontal and vertical temperature gradient is maintained to generate supersaturated conditions to form and subsequently precondition water droplets for the experiment in the Zurich Ice Nucleation Chamber (ZINC, Stetzer et al., 2008). In the top part of IMCA particles are exposed to relative humidity with respect to water of ~120% at 313 K. The high relative humidity ensures all particles transitioning through IMCA activate into cloud droplets, independent of their properties. In the lower part of IMCA, droplets containing the immersed feldspar particles are cooled to the experimental temperatures prevailing in ZINC. ZINC is a parallel plate continuous flow diffusion chamber (1 cm gap between the wall plates) layered with a thin ice layer as source of water vapour at temperatures below 273 K. The temperature of the parallel wall plates of the chamber is controlled independently by two cryostats (Lauda134 RP890). At the transition

Deleted: -

from IMCA into ZINC, additional sheath air (2 l min^{-1} on either side) is added in order to maintain the 1 mm width of the sample lamina and to prevent turbulence. Constraining the sample width to 1 mm allows to control and constrain the temperature and relative humidity that the particles are exposed to. ZINC is operated such that droplets transitioning from IMCA can be exposed to temperatures from 238 – 258 K at water saturation conditions to prevent evaporation of the droplets. After a residence time of ~10 s, water droplets and nucleated ice crystals are detected in-line (see Figure 2) by the Ice Optical Depolarization detector (IODE) described in Nicolet et al. (2010) and Lüönd et al. (2010). The water droplet and ice crystal counts at a specific temperature are used to derive the fraction of droplets that freeze due to ice nucleation on the immersed feldspar particle or by homogeneous freezing. The reported frozen fraction is defined as:

$$frozen\ fraction = \frac{\#\ ice\ crystals}{\#(ice\ crystals + water\ droplets)}$$

4. Experimental results

4.1. Temperature dependence

The shape of the temperature dependent frozen fraction is important because this dependency can dictate at which cloud supercooling one can expect particles to actively form ice and initiate glaciation in the mixed – phase cloud regime. Comparing frozen fraction shown in Figure 3 reveals different slopes of the temperature dependence for different samples as well as particle sizes. As an example, the increase in frozen fraction from 0.1 to 1 occurs over a 7 K range for 800 nm microcline particles, however this range broadens with decreasing particle size to 10 K for 100 nm particles. To illustrate this further, in Figure 4 we show the range of freezing temperatures for frozen fraction 0.1 – 1 for all 800 nm particle samples. We find that the freezing temperature range for orthoclase spreads over 10 K already for the 800 nm particles. The broader range of activation temperatures suggests that the ice nucleation active sites in the 800 nm orthoclase are more heterogeneous than the ones in the 800 nm microcline sample (see Figure 4). Additionally, we observe, that the microcline and orthoclase samples initiate freezing at warmer temperatures compared to the Na/Ca- feldspars suggesting that K-feldspars are in general more ice active in accordance with Atkinson et al. (2013). The microcline amazonite sample is the most effective sample for immersion freezing. Upon close observation of the freezing range depicted in Figure 4 however, it can be seen that the narrow freezing range is neither unique to microcline, nor the K-feldspar polymorphs as a freezing range of 5 K is also exhibited by the labradorite CH2 sample. Even though labradorite CH2 is much less ice active than orthoclase, the narrow spread in freezing temperatures suggests that the active sites of this sample are less heterogeneous than those of orthoclase.

Freezing curves for the Na/Ca-feldspars extend to temperatures where homogenous freezing sets in, suggesting that a fraction of these particles, up to 25% (considering the 800 nm particles in Figure 3), cannot nucleate ice heterogeneously. In contrast, freezing on the K-feldspars (except sanidine) occurs above the homogeneous freezing regime. Potential reasons for why

Deleted:
Deleted: (~
Deleted:)
Deleted: to

sanidine is an exception to the rest of the K-feldspars are discussed in Section 5 below. For all K-feldspar samples, the effect of temperature on the frozen fraction has a distinct size dependence where larger particle sizes exhibit a stronger temperature dependence, i.e. the change in frozen fraction with temperature is larger for large particles and smaller for small particles (see Figure 3). This can be explained by the increased probability of large particles to host at least one exceptionally efficient active site compared to smaller particles with fewer actives sites. Most plagioclase feldspar particles are ineffective heterogeneous INPs or initiate freezing only when temperatures approach homogeneous nucleation temperatures (Harrison et al., 2016).

A comprehensive analysis of how to obtain good immersion freezing parametrizations, including fitting of the microcline (amazonite) data set shown in this study can be found in Ickes et al. (2017). Parameterizations for other samples can be found in Niedermeier et al. (2015) and Peckhaus et al. (2016). Compared to the temperature dependent increase in frozen fraction predicted by a single contact angle representation within classical nucleation theory, the observed temperature dependence is less steep. This feature can be parameterized by e.g. a contact angle distribution (Ickes et al., 2017). In terms of nucleation sites per surface area (*INAS*), the number of sites increases by one order of magnitude every additional 2 K supercooling for most samples (see Fig. A1 in Appendix A). Sanidine and pericline show a weak increase of frozen fraction with decreasing temperature.

Deleted: A

4.2 Size dependence

The minimum particle size able to trigger heterogeneous ice nucleation above temperatures where droplets freeze homogeneously, is investigated within the limits of the experiment (see Section 3.1.). The range of homogeneous nucleation temperatures for water droplet sizes of 10 - 20 µm generated in IMCA was found to be 235 – 237 K (see Figure 3). The lower particle threshold size for heterogeneous ice nucleation determines how effective small inclusions, internally or externally mixed with mineral dust aerosol, will impact ice formation.

Experiments on single immersed, size-selected particles show a strong particle size dependence of ice nucleation ability. The specific slope of the median freezing temperature (T_{50}) as a function of geometric surface area varies between samples. Examples are the almost linear scaling of frozen fractions with particle size (surface area) observed for 100 - 200 nm microcline, 200 - 400 nm orthoclase and 400 - 800 nm adularia (see Figure 5). The two orthoclase (adularia) varieties, which show a low ice nucleation activity for particle sizes smaller than 200 (400) nm are observed to have a stronger increase in activity with surface area compared to the highly active samples (e.g. amazonite). This behaviour could suggest that for larger surface areas than accessible with these experiments, differences among K-feldspar species may become smaller as the T_{50} converge for the K-feldspars (Figure 5). The minimum size triggering immersion freezing is found to be 50 nm microcline particles. In particular, the amazonite sample exhibits a T_{50} of 243 K, which is higher than previously reported values of a variety of dust and clay samples (Lüönd et al., 2010; Welti et al., 2012; Kanji et al., 2013; Augustin-Bauditz et al., 2014; Hartmann et al., 2016). For most of the feldspar samples, including orthoclase and sanidine, particles of 400 or 800 nm are

required to observe effective immersion freezing, which contradicts the hypothesis of Atkinson et al. (2013), that generally tiny feldspar inclusions in dust particles will contribute to active ice nucleation. An exception is the microcline (amazonite) sample showing that even particles as small as 50 nm are able to act as INPs, suggesting that the hypothesis could be true for this K-feldspar polymorph. We note that despite the multiply charged particles expected in the 50 nm particle population (see Section 3.1), particles of this size substantially contribute to the frozen fractions observed as shown in Figure C1 (Appendix C).

Deleted: As an example, the presence of K-feldspar in the labradorite AU sample might explain its slightly higher ice nucleation activity compared to the otherwise very similar labradorite CH2 (see Figures 1 and 3).

5. Discussion

The feldspar samples used in this study show a large variability in ice nucleation temperatures. Here, we discuss properties of the feldspar group that could help to explain and categorize this variability. Pruppacher and Klett (1997) list five requirements of an ice nucleating substance: insolubility, active sites, size, ability to form chemical bond with water and crystallographic similarities to ice. For the analysis of our experiments, we can deduce the following: (a) the insolubility of feldspar on the time-scale of the experiment is reasonable to assume, (b) active sites could be chemical, crystallographic or morphological features discussed in Section 5.1. and (c) the particle size effect on ice nucleation in the immersion mode as already discussed in Section 4.2. We therefore explore the chemical composition and crystallography of the samples as ice nucleation requirements in the following.

Deleted: From

Deleted: conclude

Deleted: it remains unknown

Deleted: what particle property other than chemistry and crystallography or morphological features (Section 5.1, see Figure 6) could be active sites is discussed in Section 5.1 (see Figure 6), and

Deleted: is

5.1. Crystal structure and surface texture

None of the K-feldspar samples exhibits a close lattice match (see Table 2) to hexagonal ice Ih (a=4.52 Å, c=7.35 Å) or cubic ice Ic (a=6.35 Å), typically found at lower temperatures. There are two crystal structures in the feldspar samples tested, monoclinic and triclinic. While Na/Ca-plagioclase are all triclinic, the K-feldspar sanidine and orthoclase have a monoclinic crystal lattice. Microcline is a triclinic K-feldspar. Triclinic microcline forms by transformation of monoclinic K-feldspar upon cooling (see e.g. Waldron et al., 1993) or as suggested by Collins and Collins (1998) by K-replacement of Na/Ca-feldspar. The lattice angles of monoclinic and triclinic K-feldspar polymorphs are summarized in Table 2. It can be seen that structural differences among feldspars are small even when comparing triclinic to monoclinic lattice angles. Mason and Maybank (1958) reported experiments on triclinic microcline and monoclinic orthoclase. While microcline was found to be active at -9.5 °C their orthoclase sample was inactive above -18 °C. The data shown in Figure 3 supports a difference in ice nucleation temperature of these K-feldspars, with microcline forming ice at higher temperatures than the monoclinic orthoclase, although the absolute temperatures differ from Mayson and Maybank (1958), because of the single particle nature of our studies. In addition, the least efficient K-feldspar sample sanidine, is monoclinic. The hypothesis that within the K-feldspar polymorph, a triclinic crystal structure is a more active ice nucleation property, was reported by Augustin-Bauditz et al. (2014), based on their indirect observation that mixed dust samples containing orthoclase were less ice active than a microcline sample. However, given that orthoclase is much more ice active than sanidine (Figure 3) and both have a monoclinic structure, their

Deleted: ,

difference in ice activity cannot be explained by the crystal lattice alone. Another difference between monoclinic and triclinic K-feldspars is the order/disorder of Al^{3+} and Si^{4+} in the tetrahedral sites building the crystal structure. Monoclinic sanidine retains a disordered crystal structure (although often forms defect-free crystals) while microcline transforms to an ordered crystal. Orthoclase has intermediate disorder in this regard. The polymorphs of K-feldspar are distinguished by the randomness of this order distribution, which depends on the temperature and cooling rate during rock formation. The sequence of feldspar melting temperatures given in Lutgens et al. (2014) are Ca-feldspar>Na/Ca-feldspar>Na-feldspar>K-feldspar (sanidine>orthoclase>microcline). While Ca-feldspar is completely ordered, Na-feldspar can have varying degrees of order and Na/Ca-feldspars are disordered. The melting points of K-feldspar correspond to the ascending order of the observed T_{50} and the degree of order-disorder, indicating that ordered feldspar crystals are more active INPs than disordered crystals. However, since the crystal structures do not match that of ice, it is not possible to state what the reason for such a correlation could be.

The surface texture of the nine samples was investigated by scanning electron microscopy (SEM). Representative images are shown in Figure 6. Steps, lamellae and clustering are prominent features. Smaller particle sizes appear smoother and rounder. Due to the triclinic structure of Na/Ca-feldspar, twinning (i.e. symmetrical intergrowth, phase exosolution or Na-K exchange between feldspar phases) with triclinic microcline is common (David et al., 1995; Parsons et al., 2015; Whale et al., 2017). However, given the α and γ crystallographic angles are very close to 90° (see Table 2), it is difficult to detect twinned structures in SEM images since the surface would need to be slightly tilted (Lee et al., 1998 and references therein). The surface sites where transitioning between microcline and plagioclase occurs has been proposed to be a topological feature critical for ice nucleation (Whale et al., 2017). All K-feldspar exhibit perthitic structures (lamellae) whereas on the plagioclase feldspars this feature is less prominent or missing (Whale et al., 2017). In Figure 6, the layering from the lamellae is clearly visible for panels a - e (K-feldspars) whereas for panels f – i the layering is less visible and even absent for panels g and h (pericline and labradorite CH2). It has been reported that K-feldspar contains macropores of 0.1-1 µm diameter (David et al., 1995; Lee et al., 1995). Hodson (1998) found that the contribution of internal surface structures such as pores to the total particle surface increases with decreasing particle size for some K-feldspars (e.g. sanidine) whereas no particle size relation to pore surface was found for other samples such as microcline. For the current study the internal surface area is not of interest since in comparison to the outer surface in contact with the water droplet, ice formation is depressed in narrow confinements (Marcolli, 2014). Therefore, using the particle surface area available to nitrogen adsorption (BET-surface) as a measure of surface area might overestimate the available surface for immersion freezing nucleation. Geometric surface area assuming spherical shape is used instead (Figure 5). In none of the SEM images, intact pores are visible. This is possibly because of the Pt-coating prior to imaging. Also the grinding process applied to the samples may have eliminated this feature, as cavities and macropores of this size present favoured sites of fracture. Lamellae could stem from split pores. Before milling, the K-feldspar samples used here were translucent to opaque, indicating that they have reacted pervasively with a fluid causing exsolution and thus the perthitic structure is expected (Parsons et al., 2015). All samples were subject to the same preparation (grinding) procedure.

Deleted: s

The assumption that physical properties (e.g. hardness) are comparable among the tested feldspar species implies that the same degree of artificial surface features are introduced to all samples. The vast difference in ice nucleation efficiency between the feldspars suggests that any grinding artefacts (such as fractures or exposing high-energy surfaces) did not create ice nucleating properties, as otherwise all samples would have more comparable ice nucleation activities. Zolles et al. (2015) tested the effect of milling on a sample of microcline, albite and andesine and found none, or only a minor increase of 1K on the median freezing temperature. We note that this is not the case for all minerals as a large influence of milling has been noted for hematite (Hiranuma et al., 2014).

5.2. Chemical composition

The individual samples have been analysed by XRF spectroscopy for their bulk chemical composition and trace elements (see Table 3). Using actively ground samples from a homogeneous base material should preclude large variations in chemical composition with particle size for the samples investigated here (see INAS densities in Appendix A). A statistical classification of the XRF results using Random Forest analysis (Liaw and Wiener, 2002) to identify the important compositional predictors of T_{50} revealed Pb, Rb and Sr to be most relevant. Pb and Rb are highly positively correlated (r = 0.91), whereas the concentration of Sr in the samples shows a negative correlation to Pb (r = -0.66) and Rb (r = -0.51). The best linear correlation between a single compound and the ice nucleation activity based on T_{50}, was found for the Pb content in the feldspar samples (Figure 7). However, there is an exception with using Pb as the single compound predictor since the microcline sample has a lower lead content than the orthoclase but a higher T_{50}. Cziczo et al. (2009) have shown that the presence of Pb could increase the ice nucleation activity of dust (clay) particles. However, high Pb content alone is insufficient to explain the ice nucleation activity of a mineral dust sample in general. As an example, the ice nucleation activity of a weathering product of feldspars, kaolinite, does not appear to depend on its Pb content. XRF analysis of the kaolinite samples used in the experiments reported in Welti et al. (2012) which had a lower ice nucleation activity than microcline, revealed a ~10 fold higher Pb content (2888.4 ppm) in comparison to e.g. the amazonite sample (247.0 ppm). The high Pb content measured in kaolinite could be a result of its high adsorption capacity for Pb (Jiang et al., 2010) and can be introduced at any point after the weathering from feldspar to kaolinite. Based on these arguments and that the correlation of Pb content to T_{50} is not monotonic (e.g., lower Pb content in microcline than orthoclase, Figure 7) we focus on other predictors suggested by the Random Forest analysis.

The strongest chemical predictor for T_{50} was found to be a high Rb/Sr ratio. Contrary to the Pb content, a higher Rb/Sr monotonically corresponds to a higher T_{50} for all samples and particle sizes, shown in Figure 8. Initially each feldspar has a specific Rb/Sr partitioning influenced by its K content, the melt temperature from which it crystallized and its melt composition. If it is subsequently changed, the Rb/Sr ratio can be an indication for mineralization processes (Plimer and Elliott, 1979). Due to their ionic radii, electronegativity and ionization potentials, Rb^+ replaces K^+ while Sr^{2+} is incorporated in the feldspar crystal instead of Ca^{2+}. The Rb/Sr ratio is indicative for the position of feldspar on the ternary phase diagram (Figure 1) and the absolute concentrations of trace elements depends on the cooling/crystallization process and abundance of trace

elements in particular magmatic fluid (Parsons et al., 2009). The replacement of K by Rb results in a lower microcline polymorph, and a higher Rb/Sr ratio, correlating to higher ice nucleation activity. This suggests that the observed correlation reflects a possible relationship between ice nucleation activity and feldspar microstructure. We note that a monotonic correlation between T_{50} and a Pb/Nd ratio can also be constructed, but no interpretation of the implication of such a ratio could be found in the literature and neither was Nd suggested as a predictor by the Random Forest analysis. Zolles et al. (2015) proposed an explanation of K-feldspar ice nucleation ability based on its surface chemistry. They argue that depending on the chaotrope (order-breaking) or kosmotrope (order-making) characteristic of feldspar-surface-cations which are present in the water surface surrounding the particle, they can enhance or inhibit the structuring of water and therefore the formation of the ice phase. The ions with the higher charge densities (Ca^{2+}, Na^{+}, Sr^{2+}) tend to disturb structuring of water (increase entropy) while those with lower charge density (K^{+}, Rb^{+}) have a promoting effect (decrease entropy). Following this argument, an increased Rb^{+} concentration combined with a decreased Sr^{2+} content results in a more kosmotropic and less chaotropic surface property for the ordering of water into ice. The increased ice nucleation activity with increasing Rb/Sr ratio therefore corresponds to a higher ordering and thus supports the hypothesis of Zolles et al. (2015). It would be necessary to quantify the concentration of cations required to influence water ordering to determine how influential Rb^{+} and Sr^{2+} are for ice nucleation given their trace elemental composition.

The observed discontinuities in freezing temperature with increasing particle size, for adularia and orthoclase (see Figure 3) indicate that chemical composition alone cannot explain the ice nucleation potential of all feldspar species. That the strong size dependence is observed for both orthoclase varieties (intermediate ordered crystal structures) but not for disordered sanidine, indicates that a large enough sufficiently ordered surface area is needed to initiate efficient ice nucleation. This interpretation corroborates the suggestion of Whale et al. (2017) that some perthitic structure (microtexture) associated with the strain between K- and Na-rich regions on the samples benefits ice nucleation and these can range from the nm to mm scale, varying amongst feldspar samples. The probability of such features inevitably scale with surface area, and could explain the requirement of a critical particle size (surface area) in order to exhibit ice nucleation.

Natural weathering producing small feldspar particles commonly includes contact to acidic environments, causing removal of alkalis and aluminium and formation of a silica-rich skin. Freely exposed feldspar are reported to be populated by lichens which can alter naturally occurring feldspar in an infinite number of ways (Smith, 1998). The surface properties (specific area, porosity, molecules on the surface) of freshly ground feldspar is therefore expected to be different from aged particles (Mangan et al., 2017). However, bulk composition and crystal structure can be assumed to be representative for natural feldspar. Additionally, a majority of airborne feldspar particles could be coming from phenocrysts (inclusions of feldspar in e.g. granite matrix, Lee et al., 1995), where the trace element content could be different. Aging of microcline in concentrated solutions did not impair ice nucleation activity permanently in case of near neutral solutions, however exposure to highly acidic or alkaline solutions damaged the surface inhibiting or even destroying the ice nucleation ability (Kumar et al., 2018). We note that the

Field Code Changed

Deleted:

Deleted: (increase entropy)

Deleted: (order-making)

Deleted: (order-breaking)

Deleted: However, as

Deleted: only trace elements, their direct

Deleted: effect on ice nucleation is probably negligible.

Deleted: Using actively ground samples from a homogeneous base material precludes large variations in chemical composition with particle size for the samples investigated here.

samples used in this study could have different ice nucleation properties from feldspar found in natural airborne dust because of the natural weather elements such as cold, low pH conditions resulting in a decrease in ice nucleation activity. On the other hand, high relative humidity with high NH_3/NH_4^+ conditions could enhance ice nucleation (Kumar et al., 2018). Feldspars of the same classification but from a different location could differ in immersion mode freezing properties given that feldspars can exhibit broadly similar chemistry and structure, but at the atomic level will almost certainly differ in their intra-crystal defects as well as in their trace element chemistry (Lee et al., 1998; Parsons et al., 2015) as shown in Figures 5 and 6.

Deleted:

6. Conclusions

The immersion ice nucleation properties of size selected K- and Na/Ca-feldspar particles have been investigated in the temperature range 235 – 258 K. A pronounced sample dependent effect of particle size on immersion freezing activity is observed. The analysis of composition, lattice structure and crystallographic properties of the samples in correlation to their ice nucleation behaviour suggests two indicators for the ice nucleation activity of the feldspar samples investigated here, namely, high crystal order and the abundance of certain trace elements.

Deleted: properties are important

Deleted: for

Deleted: presence

Deleted: order-making ions on the surface

The tested K-feldspar (microcline) with high crystal order is found to exhibit a higher ice nucleation activity compared to chemically similar intermediate or highly disordered K-feldspar polymorphs (orthoclase, sanidine). The lower the K-feldspar crystallization temperature, the higher the order in crystal structure, favouring formation of microcline. Accordingly, the Na/Ca-feldspar samples investigated in this study crystallized at higher temperatures and exhibit lower ice nucleation activities. Crystal structure (triclinic or monoclinic) as a template for ice nucleation is found to be not important, as was also concluded by molecular model simulations (Pedevilla et al., 2016). The best predictor of the median freezing temperature (T_{50}) is found to be the sample Rb/Sr ratio, determined by XRF. More ice nucleation active samples show higher Rb/Sr ratios, e.g., the most active microcline sample has an order of magnitude higher Rb/Sr ratio than the second-best microcline. Therefore, Rb/Sr ratios could serve as tracer for highly ice nucleation active feldspar particles or even help to differentiate sources of feldspars acting as INP at specific temperatures.

Deleted: , which exhibits the highest ice nucleation activity amongst feldspars

Deleted: However, c

Deleted: serving

Deleted: play a minor part

Deleted: A high Rb/Sr ratio indicates a high abundance of order-making ions. This property could help to differentiate sources of feldspars acting as INP at specific temperatures.

Microcline and plagioclase feldspars have been found in natural dust surface samples from deserts (Kaufmann et al., 2016) and to a lesser extent but still significant amount in airborne dust samples (Boose et al., 2016). Particle size, wind speed and turbulence determine atmospheric transport and spread of dust particles (Mahowald et al., 2014). The size dependent immersion freezing activity therefore affects the temperature range at which certain feldspar particles contribute to cloud glaciation. Size dependent measurements indicate that for the two orthoclase samples (orthoclase, adularia), ice nucleation requires active sites present on 400-800 nm sized particles but not on the smaller size fraction (100-200 nm in diameter). The size dependent results further suggest that even small microcline particles or inclusions in clay minerals could contribute substantially to the ice activity, given the smaller size fraction (50-100 nm) of microcline that formed ice above homogeneous

Deleted: at temperatures

Deleted: that required for

freezing temperatures. A possible caveat is that atmospheric ageing can change the surface of the microcline, thus rendering its ice activity dependent on the type of chemical ageing experienced. We conclude that the larger particle size required to trigger ice formation at temperatures above homogeneous freezing for other K-feldspar samples, would prevent their inclusions within mineral dust particles to increase the ice nucleation activity of airborne mineral dusts. The experiments of the present study suggest that sanidine (most abundant K-feldspar in volcanic ash) is not an active INP.

We note that the point of origin and sampling location of the feldspars used here could limit the specific ice nucleation activity to the samples presented here, because even similar polymorphs sampled in different geological landscapes are known to have different topographical features and microtextures (Lee et al., 2007). However, the results from this work demonstrate the variation in ice nucleation activity amongst one group of minerals in the sub-micron particle range.

Additional experiments with volcanic K-feldspars (sanidine varieties) might help to explain the observed differences in ice nucleation efficiency of ashes from different volcanoes (e.g., Mangan et al., 2017) could benefit model-based studies, which forecasts aerosol plumes after volcanic eruptions to guide policy for aviation safety. Ice nucleation investigations with a larger number of samples of one specific feldspar polymorph, from different source regions could help to generalise the finding that a trace elemental fingerprint can be used to predict the ice nucleation activity of feldspar samples.

Author Contributions: AW conducted the experiments and analysed the data. AW and ZAK interpreted the data. AW and ZAK wrote the manuscript with comments from UL. ZAK and UL supervised the project.

Competing Interests: The authors declare no conflict of interest

Acknowledgements: ZAK and AW acknowledge funding from the Swiss National Science Foundation (grant 200020_150169/1). We acknowledge H. Wydler for technical support. The authors acknowledge Y. Boose for helpful discussions.

Data availability: The data presented in this publication are available at the following DOI: https://doi.org/10.3929/ethz-b-000350978

Appendix A: Ice nucleation active site (INAS) densities of feldspar polymorph samples

Based on the experimental data shown in Figure 3 (Section 4), *INAS* density (n_s) scales the frozen fraction (*FF*) by the particle surface area according to:

$$n_s = \frac{ln(1 - FF)}{A}$$

Deleted: We do not believe that the sample preparation method (grinding) could have introduced new active sites on existing surfaces, but it could have resulted in exposing fresh surfaces that are more ice active than found in natural samples.

Deleted: of

Deleted: would be necessary

Deleted: findings regardless of origin and elucidate the effects of trace compounds which are very hard to disentangle from the effects of the microtextures on the observed

Deleted: Providing a systematic classification of feldspar ice activity could benefit model-based studies, which forecasts aerosol plumes after volcanic eruptions to guide policy for aviation safety.

Where A denotes the geometric surface area, calculated as $A = 4\pi\left(\frac{d}{2}\right)^2$, with d being the selected mobility diameter. We have determined these for the all the feldspar samples as shown in Figure A1.

Appendix B: Sample Mineralogy determined by X-ray Diffraction (XRD) analysis

The composition of samples investigated here were additionally determined by Rietveld refinement of powder XRD pattern. We note that this method is subjective to the fitting procedure to some degree. Results are given in Table B1.

Appendix C: Contributions of single, double and triple charged particles to the 50 nm microcline samples.

Multiple charge contribution to measured frozen fractions of size selected particles can be estimated from the initial particle size distribution, the sizes of the single-, double-, triple- charged particles and the fraction of total particle concentration that carries one, two or three charges (Wiedensohler et al., 1986). The calculation is reproduced for 50 nm Microcline below.

Charge	Mobility diameter	Fraction of total particle concentration carrying this charge	Percentage of total selected particles
+	50 nm	0.17	63
++	73 nm	0.016	30
+++	91 nm	0.0012	7

Frozen fraction (FF) can be calculated according to Eq. A1 using INAS density or by classical nucleation theory:

$$FF = 1 - \exp(-J(T) \cdot A \cdot t) \quad \text{(C1)}$$

With $J(T)$, being the nucleation rate, A, particle surface area and t, time. Using the assumption that the temperature dependent nucleation rate $J(T)$ or *INAS* density are sample specific, not particle size dependent property and that ice nucleation activity scales with particle size, the contribution of each particle size to the total frozen fraction (shown in Fig.C1) can be calculated:

$$Contribution_{50nm} = \frac{0.63 \cdot FF_{50nm}}{FF_{tot}} \quad \text{(C2)}$$

$$Contribution_{71nm} = \frac{0.30 \cdot FF_{73nm}}{FF_{tot}} \quad \text{(C3)}$$

$$Contribution_{93nm} = \frac{0.07 \cdot FF_{91nm}}{FF_{tot}} \quad \text{(C4)}$$

The result is insensitive to the nucleation rate $J(T)$ or *INAS* density used to calculate the frozen fractions, but the same $J(T)$ or *INAS* density must be used for all sizes. From Figure C1, it can be seen that even for the lowest frozen fractions more than 40% of the particles are indeed 50 nm, whereas for frozen fractions larger than 0.5, 50% or more particles are 50 nm in mobility diameter.

References

Atkinson, J. D., Murray, B. J., Woodhouse, M. T., Whale, T. F., Baustian, K. J., Carslaw, K. S., Dobbie, S., O'Sullivan, D., and Malkin, T. L.: The importance of feldspar for ice nucleation by mineral dust in mixed-phase clouds, Nature, 498, 355-358, doi:10.1038/nature12278, 2013.

Augustin-Bauditz, S., Wex, H., Kanter, S., Ebert, M., Niedermeier, D., Stolz, F., Prager, A., and Stratmann, F.: The immersion mode ice nucleation behavior of mineral dusts: A comparison of different pure and surface modified dusts, Geophys. Res. Lett., 41, 7375-7382, doi:10.1002/2014GL061317, 2014.

Bayhurst, G. K., Wohletz, K. H., and Mason, A. S.: A method for characterizing volcanic ash from the december 15, 1989, eruption of redoubt volcano, alaska, Proceedings of the first international symposium on volcanic ash and aviation safety, 1994,, 13-17,

Boose, Y., Welti, A., Atkinson, J., Ramelli, F., Danielczok, A., Bingemer, H. G., Plötze, M., Sierau, B., Kanji, Z. A., and Lohmann, U.: Heterogeneous ice nucleation on dust particles sourced from nine deserts worldwide – part 1: Immersion freezing, Atmos. Chem. Phys., 16, 15075-15095, doi:10.5194/acp-16-15075-2016, 2016.

Cziczo, D. J., Stetzer, O., Worringen, A., Ebert, M., Weinbruch, S., Kamphus, M., Gallavardin, S. J., Curtius, J., Borrmann, S., Froyd, K. D., Mertes, S., Mohler, O., and Lohmann, U.: Inadvertent climate modification due to anthropogenic lead, Nat. Geosci., 2, 333-336, 2009.

David, F., Walker, F. D. L., Lee, M. R., and Parsons, I.: Micropores and micropermeable texture in alkali feldspars - geochemical and geophysical implications, Mineral. Mag., 59, 505-534, 1995.

Engelbrecht, J. P., and Derbyshire, E.: Airborne mineral dust, Elements, 6, 241-246, doi:10.2113/gselements.6.4.241, 2010.

Harrison, A. D., Whale, T. F., Carpenter, M. A., Holden, M. A., Neve, L., O'Sullivan, D., Vergara Temprado, J., and Murray, B. J.: Not all feldspars are equal: A survey of ice nucleating properties across the feldspar group of minerals, Atmos. Chem. Phys., 16, 10927-10940, doi:10.5194/acp-16-10927-2016, 2016.

Hartmann, S., Wex, H., Clauss, T., Augustin-Bauditz, S., Niedermeier, D., Rösch, M., and Stratmann, F.: Immersion freezing of kaolinite: Scaling with particle surface area, J. Atmos. Sci., 73, 263-278, doi:10.1175/JAS-D-15-0057.1, 2016.

Hiranuma, N., Hoffmann, N., Kiselev, A., Dreyer, A., Zhang, K., Kulkarni, G., Koop, T., and Möhler, O.: Influence of surface morphology on the immersion mode ice nucleation efficiency of hematite particles, Atmos. Chem. Phys., 14, 2315-2324, doi:10.5194/acp-14-2315-2014, 2014.

Hodson, M. E.: Micropore surface area variation with grain size in unweathered alkali feldspars: Implications for surface roughness and dissolution studies, Geochim. Cosmochim. Acta, 62, 3429-3435, doi:10.1016/s0016-7037(98)00244-0, 1998.

Hovis, G. L.: Behavior of alkali feldspars - crystallographic properties and characterization of composition and al-si distribution, Am. Miner., 71, 869-890, 1986.

Ickes, L., Welti, A., and Lohmann, U.: Classical nucleation theory of immersion freezing: Sensitivity of contact angle schemes to thermodynamic and kinetic parameters, Atmos. Chem. Phys., 17, 1713-1739, doi:10.5194/acp-17-1713-2017, 2017.

Isono, K., and Ikebe, Y.: On the ice-nucleating ability of rock-forming minerals and soil particles, J. Meteorol. Soc. Jpn. Ser. II, 38, 213-230, doi:10.2151/jmsj1923.38.5_213, 1960.

Jiang, M. Q., Jin, X. Y., Lu, X. Q., and Chen, Z. L.: Adsorption of pb(ii), cd(ii), ni(ii) and cu(ii) onto natural kaolinite clay, Desalination, 252, 33-39, doi:10.1016/j.desal.2009.11.005, 2010.

Kanji, Z. A., Welti, A., Chou, C., Stetzer, O., and Lohmann, U.: Laboratory studies of immersion and deposition mode ice nucleation of ozone aged mineral dust particles, 13, 9097-9118, doi:10.5194/acp-13-9097-2013, 2013.

Kaufmann, L., Marcolli, C., Hofer, J., Pinti, V., Hoyle, C. R., and Peter, T.: Ice nucleation efficiency of natural dust samples in the immersion mode, Atmos. Chem. Phys., 16, 11177-11206, doi:10.5194/acp-16-11177-2016, 2016.

Kiselev, A., Bachmann, F., Pedevilla, P., Cox, S. J., Michaelides, A., Gerthsen, D., and Leisner, T.: Active sites in heterogeneous ice nucleation-the example of k-rich feldspars, Science, 2016.

Knippertz, P., and Stuut, J. B. W.: Mineral dust: A key player in the earth system, Springer Netherlands, 2014.

Kumai, M.: Electron-microscope study of snow-crystal nuclei, J. Meteorol., 8, 151-156, doi:10.1175/1520-0469(1951)008<0151:Emsosc>2.0.Co;2, 1951.

Kumar, A., Marcolli, C., Luo, B., and Peter, T.: Ice nucleation activity of silicates and aluminosilicates in pure water and aqueous solutions – part 1: The k-feldspar microcline, Atmos. Chem. Phys., 18, 7057-7079, doi:10.5194/acp-18-7057-2018, 2018.

Lee, M. R., Brown, D. J., Smith, C. L., Hodson, M. E., Mackenzie, M., and Hellmann, R.: Characterization of mineral surfaces using fib and tem: A case study of naturally weathered alkali feldspars, Am. Miner., 92, 1383-1394, doi:10.2138/am.2007.2453, 2007.

Lee, M. R., Hodson, M. E., and Parsons, I.: The role of intragranular microtextures and microstructures in chemical and mechanical weathering: Direct comparisons of experimentally and naturally weathered alkali feldspars, Geochim. Cosmochim. Acta, 62, 2771-2788, doi:10.1016/s0016-7037(98)00200-2, 1998.

Lee, M. R., Waldron, K. A., and Parsons, I.: Exsolution and alteration microtextures in alkali feldspar phenocrysts from the shap granite, Mineral. Mag., 59, 63-78, doi:10.1180/minmag.1995.59.394.06, 1995.

Liaw, A., and Wiener, M.: Classification and regression by randomforest, R. J., 2/3, 18-22, 2002.

Lüönd, F., Stetzer, O., Welti, A., and Lohmann, U.: Experimental study on the ice nucleation ability of size-selected kaolinite particles in the immersion mode, J. Geophys. Res.-Atmos., 115, DOI:10.1029/2009jd012959, 2010.

Lutgens, F. K., Tarbuck, E. J., and Tasa, D. G.: Essentials of geology, Pearson Education, 2014.

Mahowald, N., Albani, S., Kok, J. F., Engelstaeder, S., Scanza, R., Ward, D. S., and Flanner, M. G.: The size distribution of desert dust aerosols and its impact on the earth system, Aeolian Res., 15, 53-71, doi:10.1016/j.aeolia.2013.09.002, 2014.

Mangan, T. P., Atkinson, J. D., Neuberg, J. W., O'Sullivan, D., Wilson, T. W., Whale, T. F., Neve, L., Umo, N. S., Malkin, T. L., and Murray, B. J.: Heterogeneous ice nucleation by soufriere hills volcanic ash immersed in water droplets, PLoS One, 12, 11, doi:10.1371/journal.pone.0169720, 2017.

Marcolli, C.: Deposition nucleation viewed as homogeneous or immersion freezing in pores and cavities, Atmos. Chem. Phys., 14, 2071-2104, doi:10.5194/acp-14-2071-2014, 2014.

Mason, B. J., and Maybank, J.: Ice-nucleating properties of some natural mineral dusts, Q. J. Roy. Meteor. Soc. , 84, 235-241, 1958.

Nesse, W. D.: Introduction to mineralogy 3rd ed., Oxford University Press, 2016.

Nicolet, M., Stetzer, O., Lüönd, F., Möhler, O., and Lohmann, U.: Single ice crystal measurements during nucleation experiments with the depolarization detector iode, Atmos. Chem. Phys., 10, 313-325, doi:10.5194/acp-10-313-2010, 2010.

Niedermeier, D., Augustin-Bauditz, S., Hartmann, S., Wex, H., Ignatius, K., and Stratmann, F.: Can we define an asymptotic value for the ice active surface site density for heterogeneous ice nucleation?, J. Geophys. Res., 2014JD022814, doi:10.1002/2014JD022814, 2015.

Ostrooumov, M., and Banerjee, A.: Typomorphic features of amazonitic k-feldspar from the keivy granitic pegmatite (kola peninsula, russia), Schweiz. Mineral. Petrogr. Mitt., 85, 89-102, 2005.

Parsons, I., and Boyd, R.: Distribution of potassium feldspar polymorphs in intrusive sequences, Mineral. Mag., 38, 295-311, doi:10.1180/minmag.1971.038.295.03, 1971.

Parsons, I., Gerald, J. D. F., and Lee, M. R.: Routine characterization and interpretation of complex alkali feldspar intergrowths, Am. Miner., 100, 1277-1303, doi:10.2138/am-2015-5094, 2015.

Parsons, I., Magee, C. W., Allen, C. M., Shelley, J. M. G., and Lee, M. R.: Mutual replacement reactions in alkali feldspars ii: Trace element partitioning and geothermometry, Contrib. Mineral. Petrol., 157, 663-687, doi:10.1007/s00410-008-0358-1, 2009.

Peckhaus, A., Kiselev, A., Hiron, T., Ebert, M., and Leisner, T.: A comparative study of k-rich and na/ca-rich feldspar ice-nucleating particles in a nanoliter droplet freezing assay, Atmos. Chem. Phys., 16, 11477-11496, doi:10.5194/acp-16-11477-2016, 2016.

Pedevilla, P., Cox, S. J., Slater, B., and Michaelides, A.: Can ice-like structures form on non-ice-like substrates? The example of the k-feldspar microcline, J. Phys. Chem. C. , doi:10.1021/acs.jpcc.6b01155, 2016.

Plimer, I. R., and Elliott, S. M.: Use of rb-sr ratios as a guide to mineralization, J. Geochem. Explor., 12, 21-34, doi:10.1016/0375-6742(79)90060-8, 1979.

Pruppacher, H. R., and Klett, J. D.: Microphysics of clouds and precipitation, 2nd Edition ed., Kluwer, Dordrecht, 976 pp., 1997.

Pruppacher, H. R., and Sänger, R.: Mechanismus der vereisung unterkühlter wassertropfen durch disperse keimsubstanzen, Z. Angew. Math. Phys. , 6, 485-493, doi:10.1007/BF01600534, 1955.

Rosinski, J.: Role of natural and man-made ice-forming nuclei in the atmosphere, Adv. Colloid Interface Sci., 10, 315-367, doi:10.1016/0001-8686(79)87010-4, 1979.

Schumann, U., Weinzierl, B., Reitebuch, O., Schlager, H., Minikin, A., Forster, C., Baumann, R., Sailer, T., Graf, K., Mannstein, H., Voigt, C., Rahm, S., Simmet, R., Scheibe, M., Lichtenstern, M., Stock, P., Ruba, H., Schauble, D., Tafferner, A., Rautenhaus, M., Gerz, T., Ziereis, H., Krautstrunk, M., Mallaun, C., Gayet, J. F., Lieke, K., Kandler, K., Ebert, M., Weinbruch, S., Stohl, A., Gasteiger, J., Gross, S., Freudenthaler, V., Wiegner, M., Ansmann, A., Tesche, M., Olafsson, H., and Sturm, K.: Airborne observations of the eyjafjalla volcano ash cloud over europe during air space closure in april and may 2010, Atmos. Chem. Phys., 11, 2245-2279, doi:10.5194/acp-11-2245-2011, 2011.

Smith, J. V.: Atmospheric weathering and silica-coated feldspar: Analogy with zeolite molecular sieves, granite weathering, soil formation, ornamental slabs, and ceramics, Proc. Natl. Acad. Sci. U. S. A., 95, 3366-3369, doi:10.1073/pnas.95.7.3366, 1998.

Stetzer, O., Baschek, B., Luond, F., and Lohmann, U.: The zurich ice nucleation chamber (zinc) - a new instrument to investigate atmospheric ice formation, Aerosol Sci. Technol., 42, 64-74, doi:10.1080/02786820701787944, 2008.

Waldron, K., Parsons, I., and Brown, W. L.: Solution-redeposition and the orthoclase-microcline transformation - evidence from granulites and relevance to o-18 exchange, Mineral. Mag., 57, 687-695, doi:10.1180/minmag.1993.057.389.13, 1993.

Welti, A., Lüönd, F., Kanji, Z. A., Stetzer, O., and Lohmann, U.: Time dependence of immersion freezing: An experimental study on size selected kaolinite particles, Atmos. Chem. Phys., 12, 9893-9907, doi:10.5194/acp-12-9893-2012, 2012.

Whale, T. F., Holden, M. A., Kulak, A. N., Kim, Y.-Y., Meldrum, F. C., Christenson, H. K., and Murray, B. J.: The role of phase separation and related topography in the exceptional ice-nucleating ability of alkali feldspars, Phys. Chem. Chem. Phys., 19, 31186-31193, doi:10.1039/C7CP04898J, 2017.

Wiedensohler, A., Lutkemeier, E., Feldpausch, M., and Helsper, C.: Investigation of the bipolar charge-distribution at various gas conditions, J. Aerosol. Sci., 17, 413-416, doi:10.1016/0021-8502(86)90118-7, 1986.

Yakobi-Hancock, J. D., Ladino, L. A., and Abbatt, J. P. D.: Feldspar minerals as efficient deposition ice nuclei, Atmos. Chem. Phys., 13, 11175-11185, doi:10.5194/acp-13-11175-2013, 2013.

Zimmermann, F., Weinbruch, S., Schutz, L., Hofmann, H., Ebert, M., Kandler, K., and Worringen, A.: Ice nucleation properties of the most abundant mineral dust phases, J. Geophys. Res.-Atmos., 113, doi:10.1029/2008jd010655, 2008.

Zolles, T., Burkart, J., Hausler, T., Pummer, B., Hitzenberger, R., and Grothe, H.: Identification of ice nucleation active sites on feldspar dust particles, J. Phys. Chem. A. , 119, 2692-2700, doi:10.1021/jp509839x, 2015.

Table 1. Sample specification of feldspars used in this study.

Sample name	Source region	Feldspar type	Crystal structure
Orthoclase	Italy (Elba)	K	Monoclinic
Adularia	Switzerland	K	Monoclinic
Sanidine	Germany	K	Monoclinic
Microcline	Italy (Elba)	K	Triclinic
Microcline (Amazonite)	Namibia	K	Triclinic
Labradorite AU	Austria	Na/Ca	Triclinic
Pericline (Albite)	Switzerland	Na	Triclinic
Labradorite CH2	Switzerland	Na/Ca	Triclinic
Labradorite CH1	Switzerland	Na/Ca	Triclinic

Table 2. Lattice parameters for K-feldspar polymorphs from Hovis (1986) and Ostrooumov and Banerjee (2005).

Feldspar type	a (Å)	b (Å)	c (Å)	α (deg)	β (deg)	γ (deg)
Microcline	8.59	12.97	7.22	90.6	116	87.8
Amazonite	8.59	12.97	7.22	90.9	116	87.6
Orthoclase	8.60	13.00	7.20	90	116	90
Adularia	8.60	12.97	7.21	90	116	90

Sanidine	8.60	13.02	7.18	90	116	90

Table 3. Chemical analysis from XRF of the different feldspar samples used in this study. N/D stands for not detectable but could be above zero. A zero implies reliable absence of a compound.

	Plagioclase Feldspar				Potassium Feldspar				
	Labradorite CH1	Labradorite CH2	Labradorite AU	Pericline (Albite)	Adularia	Sanidine	Orthoclase	Microcline	Amazonite
Compound	**wt %**								
SiO_2	55.05	56.809	60.429	73.471	64.035	64.51	64.841	64.794	65.357
TiO_2	0.095	0.117	0.192	0.005	0.008	0.017	0.06	0.005	0.005
Al_2O_3	27.915	26.404	23.366	16.524	18.87	18.753	18.742	18.618	18.490
Fe_2O_3	0.254	0.39	0.554	0.027	0.032	0.177	0.268	0.044	0.041
MnO	0.006	0.006	0.009	0.002	0.001	0.002	0.005	0.004	0.003
MgO	0.007	0.087	0.216	0	0	0	0.11	0	0
CaO	10.415	8.224	6.702	0.055	0	0.041	0.392	0.064	0.019
Na_2O	5.148	6.591	5.32	9.918	0.978	1.719	2.337	1.836	2.551
K_2O	0.587	0.21	1.004	0.014	14.749	13.94	12.176	13.965	12.588
P_2O_5	0.017	0.05	0.035	0.007	0.004	0.035	0.036	0.026	0.008
Cr_2O_3	0.001	0.001	0.007	N/D	N/D	N/D	0.001	N/D	0.001
LOI	0.4	0.86	2.006	0.526	0.407	0.293	0.62	0.58	0.384
Total	99.894	99.75	99.84	100.549	99.084	99.487	99.587	99.936	99.447
Element	**Traces (ppm)**								
Rb	0.9	0	14.6	3	426.1	208.8	459	460.9	4566.8
Ba	161.2	225.9	180.7	0	10591.7	4883.4	1812.6	198.6	324.8
Sr	991.9	1567.5	746.4	274.2	720.6	1236.6	295.2	42.9	30.7
Nb	1.3	2.8	3.7	3.2	1.7	3.3	2.9	1.8	8.9
Zr	0	0	30.4	0	0	0	34.6	0.7	2.2
Hf	5.2	6.4	5.1	2.4	3.8	5.6	3.8	2.8	0.0
Y	2.8	2.9	6	0.3	0	0.4	0	0	0.0
Ga	29.7	24.4	25.7	15.3	19	27.4	26.8	24.2	91.6
Zn	10.6	7.8	13.4	2.7	5.2	7.2	11.6	5.8	10.4
Cu	6.8	20.6	121.1	0	33	94.5	75.4	3.9	1515.4
Ni	0.8	3.8	3.3	0	0.7	0	0.9	0	0.4
Co	21.3	40.6	1.3	43.7	21.6	14.5	16.2	32.5	13.6
Cr	5.1	8.8	51.7	2.2	2.1	2.8	8.9	2.6	5.7
V	4.3	4.4	13.3	1.8	3.8	3.1	3.6	1.9	10.1
Sc	0	0	1.2	0	0	0	3	0.6	1.8

Deleted: FeO

Deleted: .000

Deleted: NiO

La	0	1.3	7.9	7.4	0	0	13.8	3.1	82.2
Ce	0	0	22.8	0	64.7	22.5	32	0	3.3
Nd	9	6.4	16.6	8.1	32.4	17	19.6	8.4	8.7
Pb	19.1	18.7	11.4	10.2	80.5	21.3	135.7	90.5	247.0
Th	0	0	2.9	0.8	0	0	7.7	0.2	0.0
U	0	0	0	0	0	0	0.5	0	2.1

Table B1. Mineralogical composition (mass %) of feldspar samples as determined by powdered XRD using the Rietveld Refinement method.

Sample	orthoclase	adularia	sanidine	microcline	plagioclase	quartz	Others
Orthoclase	70				15	5	10
Adularia		100					
Sanidine			100				
Microcline				90	10		
Microcline (Amazonite)				77	22	1	
Labradorite (AU)					59	12	29
Pericline					84	16	
Labradorite CH2					100		
Labradorite CH1					100		

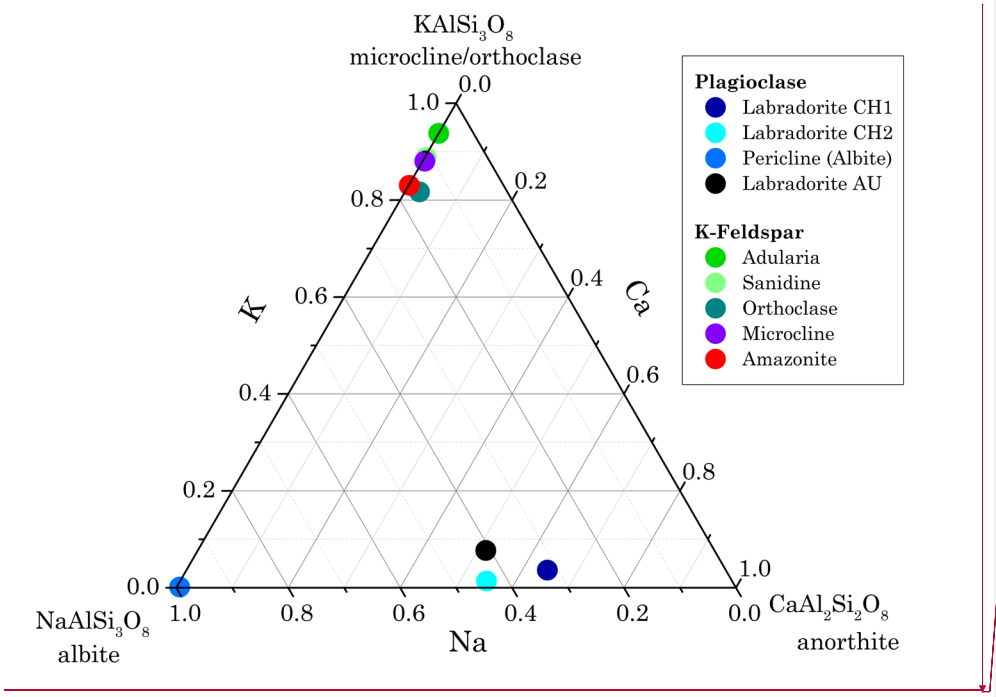

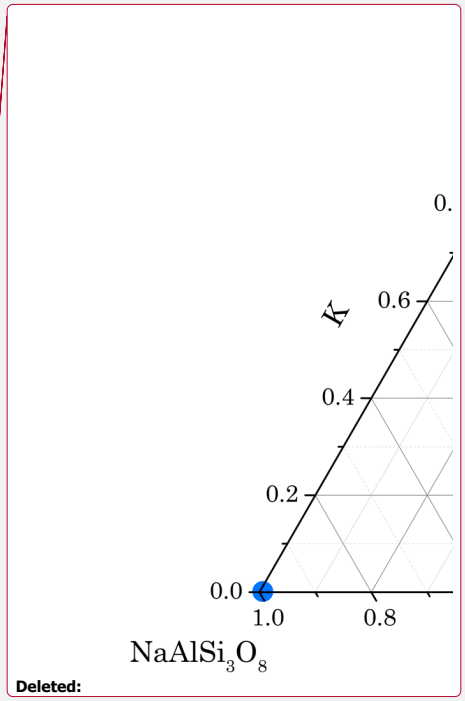

Deleted:

Figure 1. Phase diagram of feldspar samples investigated. Composition determined from X-ray fluorescence spectroscopy (XRF).

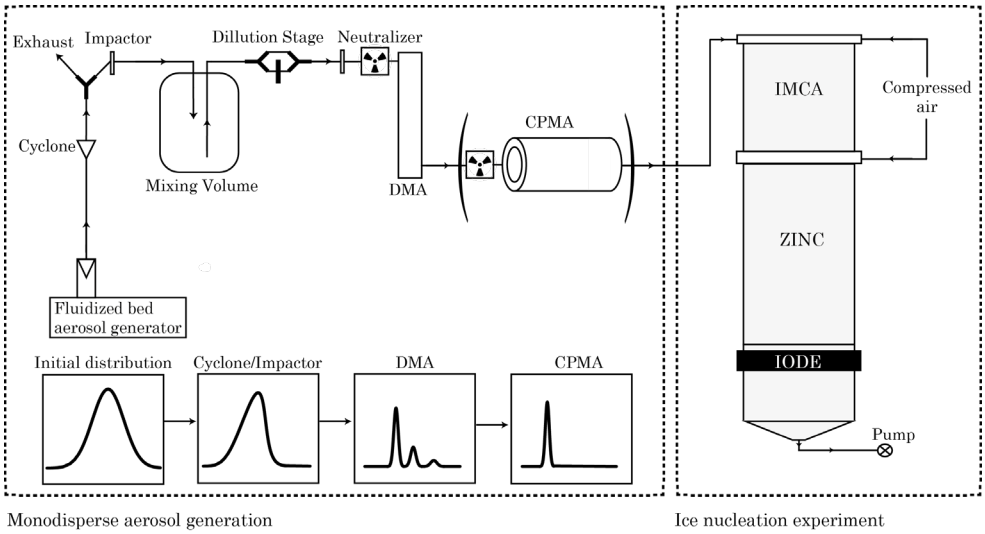

Figure 2. Schematic of the particle generation and ice nucleation set-up used to examine immersion freezing of the feldspar samples.

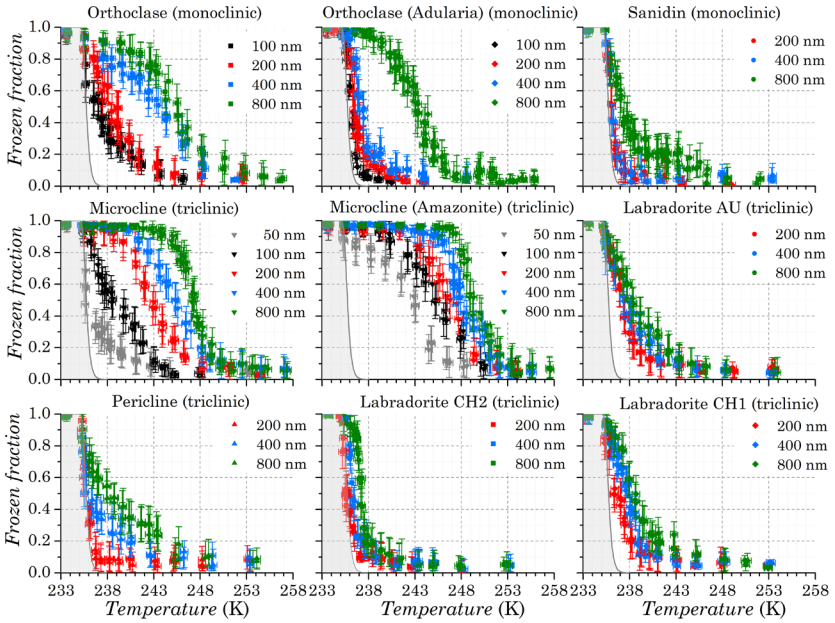

Figure 3. Frozen fractions of size selected feldspar polymorphs. The frozen fraction of water droplets due to homogenous freezing in the setup is given by the grey shaded area. Smaller particles (50 and 100 nm) were only tested for the more ice active samples. Horizontal error bars represent the variation in the sample temperature across the aerosol layer in ZINC and vertical error bars represent uncertainty in the measured frozen fraction due to overlap in depolarization ratio of droplets and ice crystals in the IODE signal (Lüönd et al., 2010).

Deleted: E

Deleted: ice crystals (top) and water droplets (bottom) and determine according to the description in section 3.2.

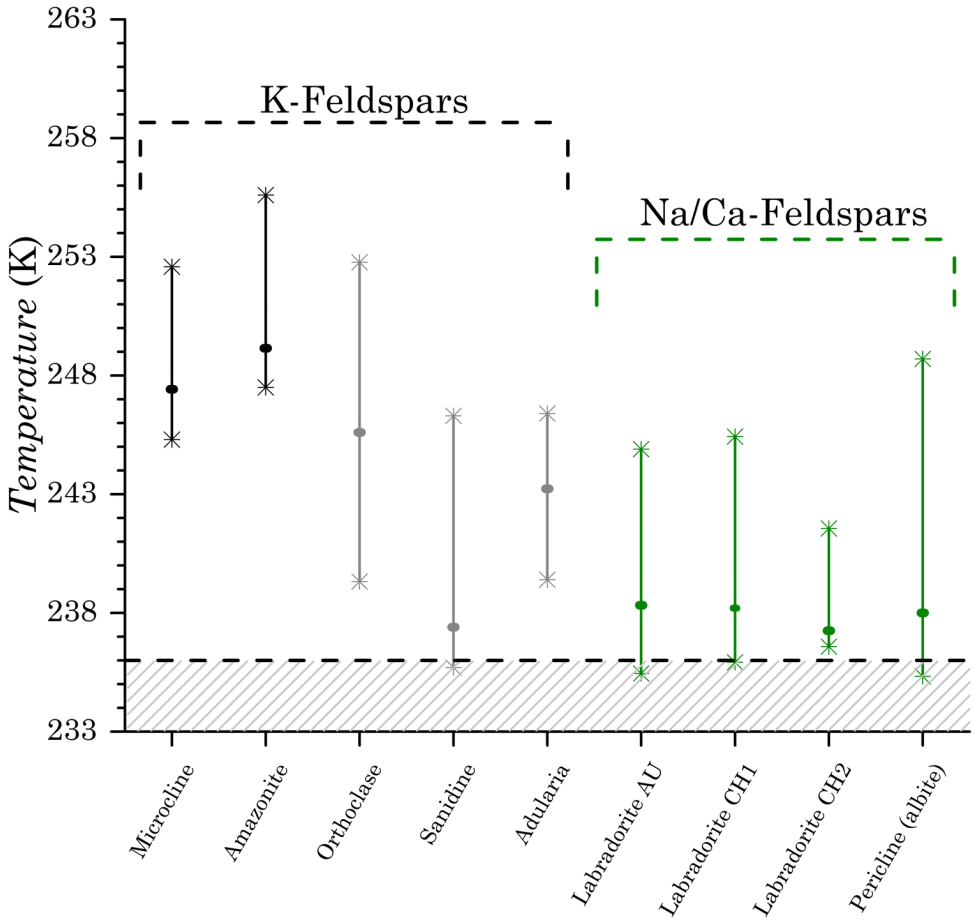

Figure 4. Spread in freezing temperatures corresponding to frozen fraction of 0.1 to 1, for 800 nm feldspar particles. Hashed region indicates homogeneous freezing as the dominant mechansim.

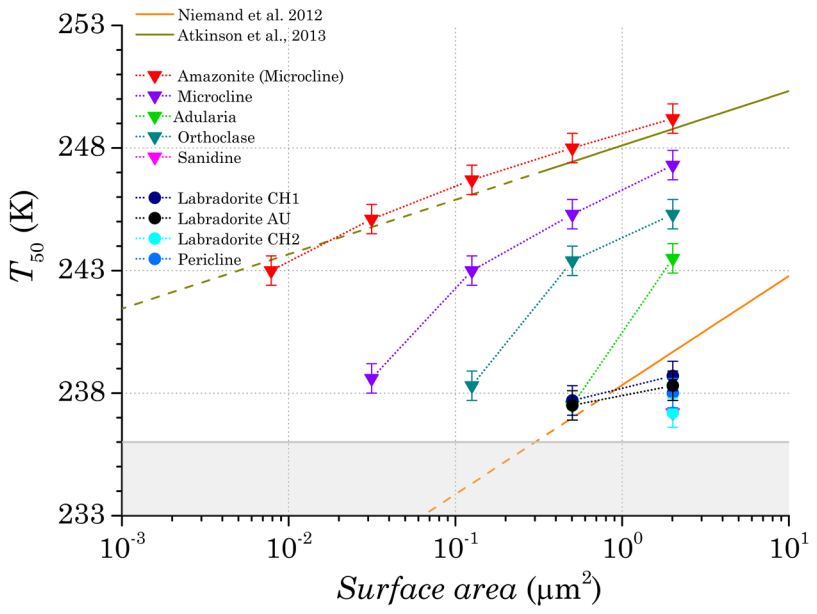

Figure 5. Median freezing temperature (T_{50}) where 50% of particles are observed to be frozen as a function of geometric particle surface area. Parameterizations for desert dust from Niemand et al. (2012) and K-feldspar from Atkinson et al. (2013) are included for comparison. Dashed lines indicate extrapolation of the parameterization to lower temperatures. Frozen fractions where T_{50} was not reached above homogeneous freezing temperatures, have been excluded.

Deleted:

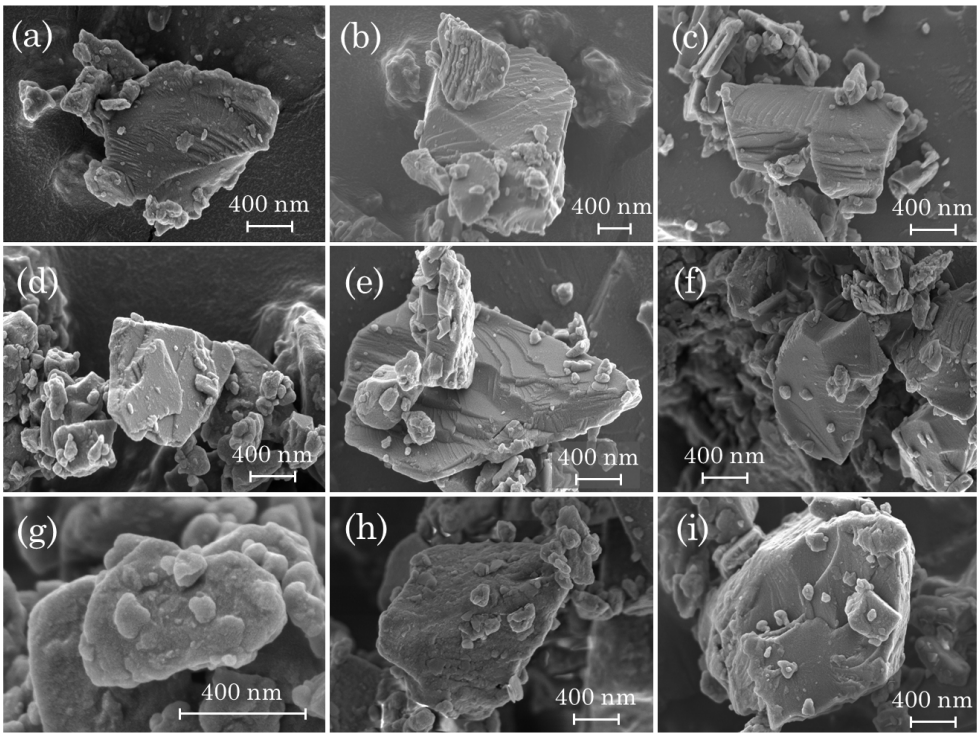

Figure 6. Representative scanning electron microscope images of (a) Orthoclase, (b) Adularia, (c) Sanidine, (d) Microcline, (e) Amazonite, (f) Labradorite AU, (g) Pericline, (h) Labradorite CH2, (i) Labradorite CH1. For reference, the 400 nm scales are indicated in the figures. The lamellae (perithitic) structure can be seen for the K-feldspars (a-e) and to a lesser extent for the plagioclase feldspars (f – i), but is almost absent for pericline (g) and Labdradorite CH2 (h). Images taken using a LEO 1530 Gemini SEM. Dust samples were applied to adhesive, carbon conductive tapes and sputter coated by a thin platinum layer. High-resolution secondary electron (in-lens SE detector) images were acquired at 2 kV.

Deleted: is clear

Deleted: less obvious

Deleted: d

Deleted: , but

Deleted: even

Deleted:

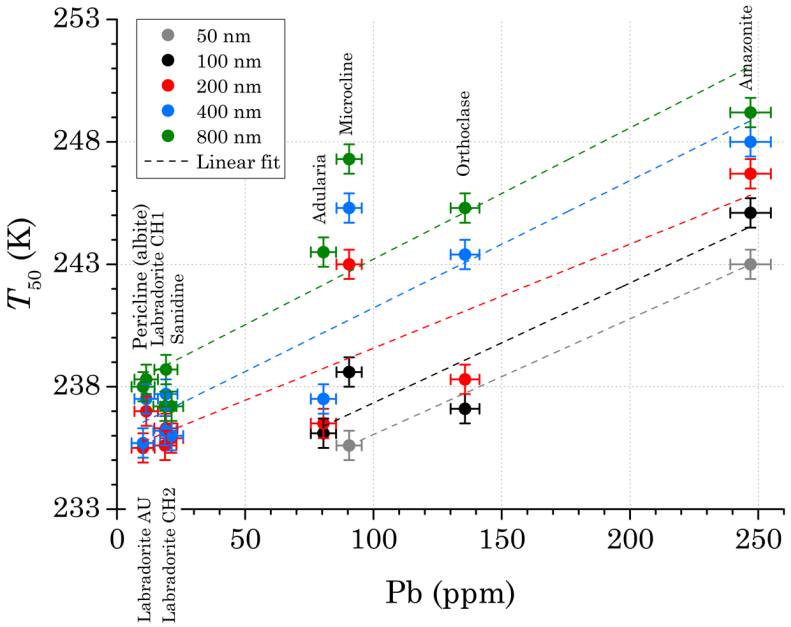

Figure 7. Particle-size dependent median freezing temperature (T_{50}) as a function of lead (Pb) content. Particle-size is indicated by the colored legend.

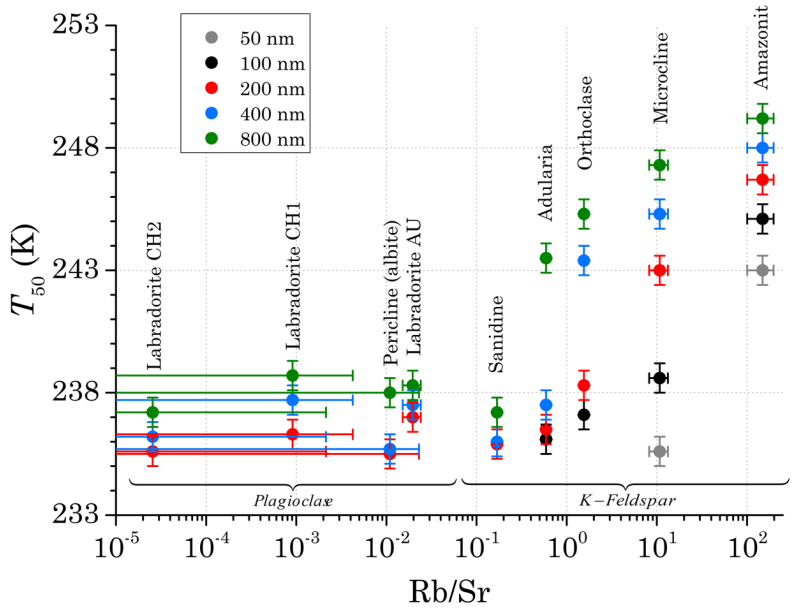

Figure 8. Particle-size dependent median freezing temperature (T_{50}) as a function of the Rb (rubidium)/Sr (strontium) ratio. Particle-size is indicated by the colored legend.

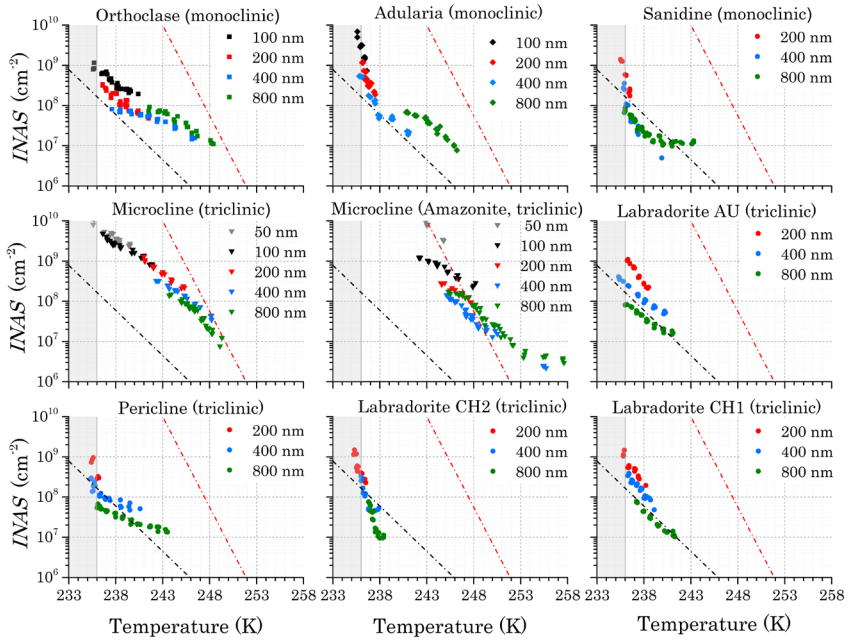

Figure A1. ***INAS*** **densities of 9 feldspar samples as a function of temperature and size corresponding to observed frozen fractions as shown in Figure 3. The upper (80-100%) and lower (0-20%) frozen fractions have been omitted to exclude saturation errors from the detection.**

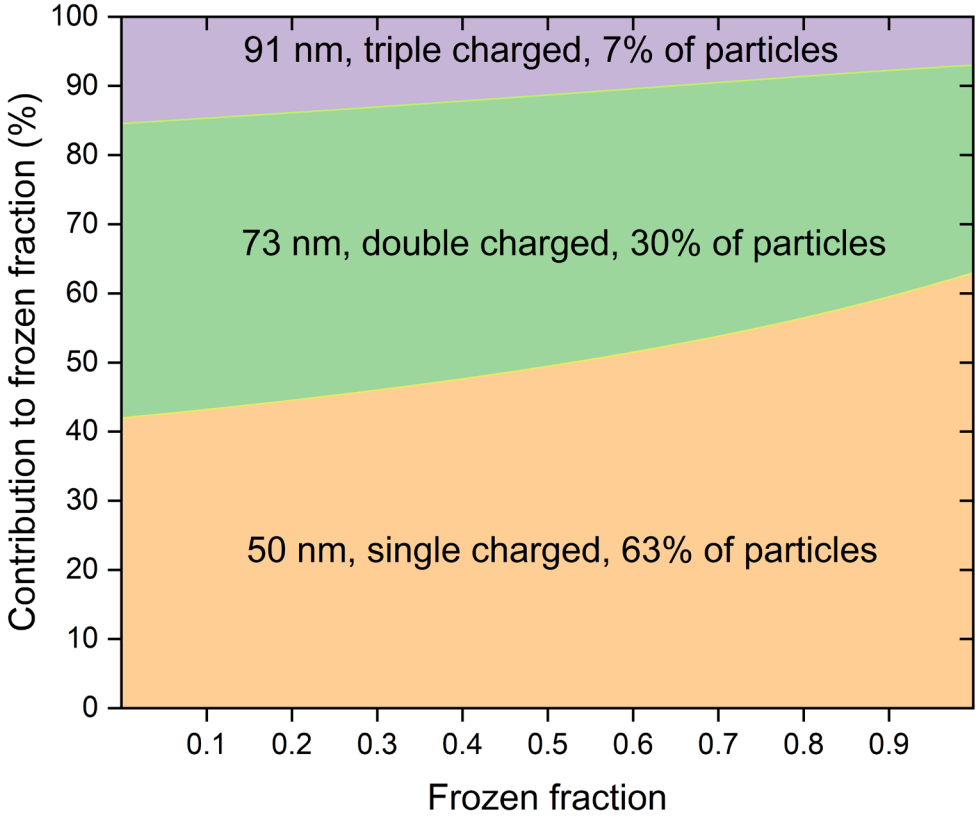

Figure C1. Contribution of single, double and multiply charged particles to the frozen fraction of 50 nm Microcline and Amazonite samples.